ALKOR-Berichte

Baltic Sea Geophysical Student Field Trip

Cruise No. AL527

06.09.2019 – 14.09.2019
Kiel (Germany) – Kiel (Germany)

Sebastian Krastel, Christian Berndt, Jens Schneider v. Deimling, Kai-Frederik Lenz, Philipp Held, Michael Kühn, Per Oscar Nilsson, Anna Christina Hans, Tatjana Michaela Weiler, Jonas Liebsch, Theresa Prigan, Tilman May, Johanna Klein, Kelvin Rathjens, Pascal Koch

Sebastian Krastel
Christian-Albrechts-Universität zu Kiel

2019

Contents

1 Preface

Cruise AL527 was carried out as a marine geophysical field course of Kiel University. One task for the participating students was the preparation of the cruise report. Hence, the focus of this report is on the description of methods and data acquisition but it also includes some first result. Some parts of the report are not written in a typical way for cruise reports but we (Christian Berndt, Jens Schneider von Deimling, Sebastian Krastel) decided not to modify the student's report because it documents the activities of the field course.

2 Summary

The cruise AL527 took place in the Western Baltic Sea in the period 6. – 14.09.2019. The cruise was carried out as a marine geophysical field course of Kiel University, supported by BONUS ECOMAP project. Starting and ending point of the cruise was Kiel. One stopover in Kiel took place during the cruise due to an exchange of parts of the scientific party (10.09.2019). The main aim of the cruise was to introduce marine geophysical acquisition to the students including hands-on experience in collecting marine geophysical data. This approach also included a first processing and interpretation of the data as well as the presentation of the first results.

Two areas in the Western Baltic Sea were the main working areas of AL527. The first survey area was at Boknis Eck, a part of the Eckernförde Bay. The main objective in this area was to search for an underwater observatory from the Coastal Observing System for Northern and Arctic Seas Project (COSYNA), which was operated by GEOMAR and disappeared end of August 2019. For this purpose, a survey with a bathymetric multibeam system from the ”Marine Geophysics and Hydroacoustics” working group (Kiel University) was carried out. Furthermore, an underwater camera system was used for visual inspections. The second survey area was in the Mecklenburger Bay. The main objective was a pre-investigation of a buried beach for an upcoming cruise within the EU-funded project ACT-SENSE. Therefore, 2D reflections seismic, sediment echo sounder, and multibeam data were acquired. Additionally, 7 gravity cores were taken for ground trothing and sampling of the buried beach. In order to analyze major tectonic structures in the Fehmarn Belt and the Mecklenburger Bay, 12 additional seismic profiles were collected when transiting between the survey areas.

Our investigations showed that a buried beach is located in the Mecklenburger Bay beneath a layer of mud. The sand deposits have an estimated variable thickness between 1m and 9m in the survey area. The top of the beach was successfully sampled with several gravity cores. Further investigations of these cores, together with the geophysical data, will be take place in the frame of the ACT-SENSE project.

In the acquired bathymetric dataset from Boknis Eck some conspicuous zones could be identified, where possibly remaining parts of the missing underwater observatory are located. Unfortunately, it was not possible to validate these zones by the used underwater camera. These zones should be investigated by divers in the near future, for a reliable validation.

3 Introduction

The geophysical student field training cruise AL527 took place in the german territory of the Baltic Sea, more precisely in the Bay of Eckernförde and Mecklenburg.
One of the aims of this cruise was to gather more information for the search of the lost observatory from the Coastal Observing System for Northern and Arctic Seas Project (COSYNA), which is partly shown in Figure 1 during its deployment (Baschek *et al.* , 2017). The system was installed in December 2016 and measured temperature, salinity, oxygen, nutrients and chlorophyll concentration close to Boknis Eck in the Bay of Eckernförde. The connection to the observatory was lost on the 21st of August 2019 under unknown circumstances. Research divers only found the disrupted power cable and dragging traces on the seafloor close to the initial position of the station (Römer, 2019). During this cruise we surveyed with a prototype Multibeam Echosounder (MBES), kindly provides by the EU-funded BONUS ECOMAP project. Seeing that the observatory, or its debris, has a higher accoustic backscatter intensity and is elevated from the surrounding sea floor and we applied the Multibeam technology for the search.

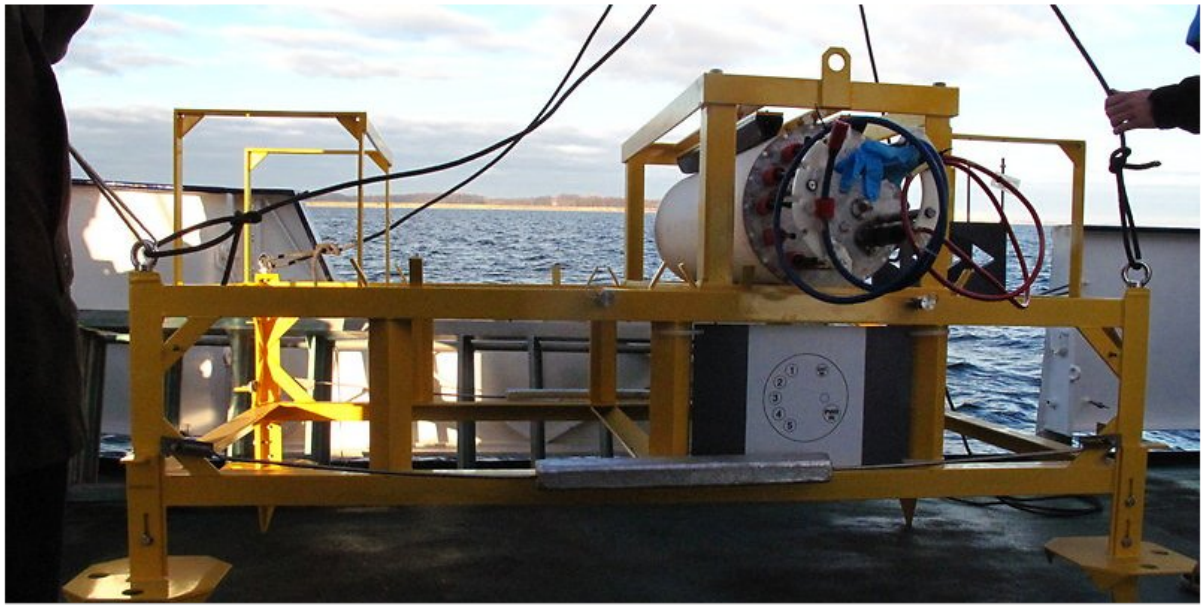

Figure 1: Picture of the missing observatory taken from Forschungstaucher (2019) of Kiel University.

A further aim of this cruise was a survey of the seafloor in the Bay of Mecklenburg as a pre-investigation for an upcoming cruise within the EU-funded project ACT-SENSE. According to the IPCC, geological storage of CO_2 is one promising method to achieve the goal of a maximum global warming by 2 °C. To avoid an unexpected aftermath, it is important to understand the impact of underwater gas injections into geological structures beforehand (Berndt, 2005). One field campaign for gaining more knowledge

about the related processes is scheduled for October 2020 (for more information (Berndt & Karstens, 2019)). It is going to take place in the area of the Bay of Mecklenburg where evidences of buried, presumably pre-glacial beaches exist (Heinrich *et al.* , 2016). The setting of sand below impermeable mud is good for gas injections. The aim of cruise AL527 was mapping of the potential injection areas by using 2D reflection seismics and hydroacoustics. Sediment samples taken by a gravity corer or a grab provide useful information to define the relevant sediment properties in preparation of the injection. The data of the Innomar Sediment Echosounder (SES) and sediment cores allow to charted the location and depth of the beach. Backscatter and bathymetry data collected by the NORBIT MBES can be used as reference data for potential injections.

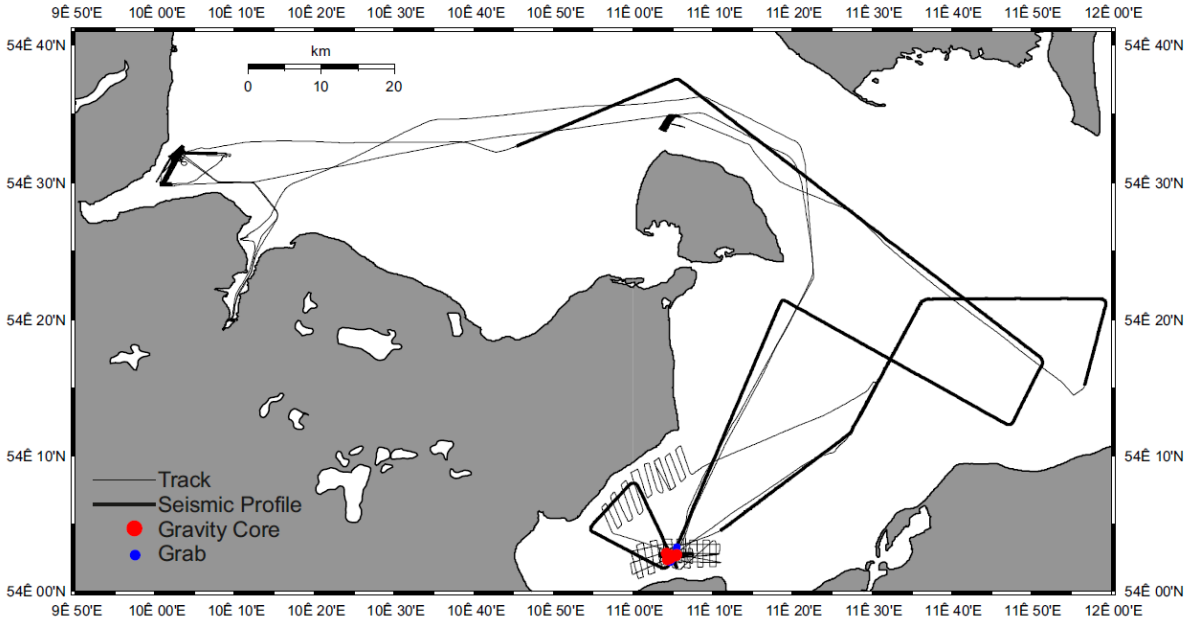

Figure 2: Cruise track of AL527. In the west the searching area for the observatory close to Boknis Eck. In the south the survey area for the measurement in the Bay of Mecklenburg. Red marks show where gravity cores were taken. Grabs are marked with blue points. Thick lines show seismic Profile tracks, and thin lines show the cruise track.

To understand the geological structure of the seafloor in the Bay of Mecklenburg, it is necessary to look at the history of the Baltic Sea. In the Perm (252 Million years ago) the Zechstein Sea was dried out repeatedly. At this time residues of evaporation deposited. The second to last layer of evaporation is made of halites. Due to its lower density, it rises to the surface. During the Triassic, layers of sandstones, carbonates, sandy maris and mudstones are typical shell limestone accumulations. Jurassic sediments are mostly interbedded sand- and mudstones. Typical sediments in the Createaeous are sandstone and carbonates. In the Cenozoic the most common deposits are mudstones (Hübscher, 2010). The formation of the Baltic Sea started in the middle Miocene after

the last glaciation. The leftover of the ice margin are glacial drifts and moraines. After this holocene, silt and sand had a thickness of about 9 m (Winterhalter, 1992).

4 Narrative of the Cruise

In the morning of the **6th of September** the scientific group consisting of four senior scientists and eight students boarded the R/V ALKOR. The scientific equipment, that had been boarded earlier, was unpacked, installed and secured. The following cruise track is shown in Figure 2. The cruise itself started shortly past 08:10am from the Geomar pier in Kiel. We reached the Bay of Eckernförde, the first research area, around noon. Upon arrival we started a Multibeam Echosounder (MBES) mattress in order to search for the lost underwater observatory of Geomar in the restricted area Hausgarten. Using Kiel University NORBIT MBES, we discovered dragging traces and anomalies on the seafloor. In between the survey a Conductivity, Temperature, Depth (CTD) profiler was deployed in order to determine a depth profile of the sound velocity for MBES calibration. We finished the survey in the early evening hours and started a 2D reflection seismic survey using a streamer with 48 channels and an active length of 75 m. The survey was planned to run throughout the night towards the Bay of Lübeck passing by four permanent environmental impact survey points. Due to decreasing pressure at the airgun, the survey was cancelled around 09:00pm, airgun and seismic streamer were recovered. The technical problem could not be solved that evening. However, it could be identified that the adapter between compressor and supply cable for the air gun was the cause. Therefore, we steamed back to the Bay of Eckernförde to perform another MBES bathymetry survey. The mattress started at 01:30am the following day, the **7th of September**. It was situated just north of Mittelgrund, intending to fill in gaps of previous surveys regarding pockmarks. After completion of the mattress another CTD was deployed. Since the adapter for the compressor of the air gun could be replaced in the morning hours, we followed up on the earlier 2D seismic survey plan and headed at 02:30pm through the Fehmarn Belt into the Bay of Mecklenburg. The survey was finalized at 03:30pm on the **8th of September**. Shortly afterwards we proceeded with a mattress north-east of Lübeck using the ship-board Innomar Sediment Echo Sounder (SES) to investigate the remainders of a pre-glacial beach. The SES survey was finalized the following day, the **9th of September**, at 02:00pm and was followed by another MBES mattress in the same area. During the survey three CTDs were deployed and a rolling calibration was applied in order to ensure data quality. We finished this survey by midnight and secured all inventory for the following transit to the Bay of Strande, where we arrived by 07:00am on the **10th of September**. At the Bay of Strande we did a short MBES mattress in order to investigate a presumed bomb crater. At 09:30am we arrived in Kiel at the Geomar pier for a partial exchange of the scientific crew and departed at 12:00am again towards the Bay of Eckernförde. At 02:00pm we performed a video camera survey at Hausgarten, the area where parts of the lost underwater observatory are assumed, according to our processing of the previously

taken MBES data. Unfortunately, visibility was weak since only little light reached the seafloor and the installed light system was insufficient. Apart from that, exact navigation was not possible with the positioning system of the R/V ALKOR. Therefore, the survey was ended at 05:30pm. Nevertheless, we had sight on parts of the instrumental tower for a couple of seconds. Within the Bay of Eckernförde we performed another MBES mattress from 05:00pm until 07:00pm, followed by an Innomar mattress on the edge of Mittelgrund in order to investigate pockmarks further. This survey was completed by 10:50pm. Afterwards we set course towards the Bay of Lübeck. The transit lasted through the night and scientific work was resumed at 08:00am the following morning, the **11th of September**. At 07:00am we started another Innomar SES survey northeast of Lübeck which lasted until 02:00pm and was interrupted twice for gravity cores. Both of the cores were taken close to shore off Brook in order to investigate the possibility of storing CO_2 within the underlying sands. One of the cores was cut open and prepared for sampling to teach the students the method and process. Afterwards, we took seven grab samples to inspect the material of the upper seafloor. This enables better and more specific interpretation of the MBES backscatter data and verifies the structures supposed by the earlier survey. By 05:00pm we began another seismic survey within the Bay of Mecklenburg in order to gather further information on the Baltic tectonics. Over the course of the evening, the wind speed increased drastically, which made us recover the streamers ahead of schedule by 09:30pm as constant data acquisition was not possible due to the swell. Therefore, we moved towards Grömitz to start another Innomar and MBES mattress at 11:45pm which was finished by 10:00am the next morning of the **12th of September**. At that time we reached the next gravity coring position, close to the former coring area northeast of Lübeck. Altogether, we covered 6 locations, taking 5 cores since the corer could not penetrate the seafloor at one of the spots. All the cores were cut and packed appropriately for further examinations by Dr. Christian Berndt's work group at Geomar. In the afternoon, by 03:00pm we carried out another seismic survey within the Bay of Mecklenburg. Seismic streamer and airgun were recovered at 11:00pm in the Fehmarnbelt. Early morning of the **13th of September**, at 03:30am we ran another MBES mattress in order to survey a ripple field off Fehmarn that is being closely watched for a few years by now. Due to wind conditions we could not take the survey as planned with profiles in roughly north-south direction but had to change to roughly east-west profiles by 08:30am. At the beginning of the survey, a CTD profile was taken from which we could not read any data for technical problems. Another CTD profile was successfully taken shortly before the survey was ended at 11:30am. Afterwards, we took four more grab samples of the upper seafloor within the area of the just finished MBES survey, slowly heading towards Kiel. In between 01:50pm and 03:50pm different presentations on preliminary results of the cruise were given. Meanwhile, we ran a last MBES survey of the western branch of the ripple field off Fehmarn. Throughout the

day, cleaning and packing of equipment had started and remained the main activity throughout the remaining transit time to Kiel. The cruise found a successful ending at 06:00pm at the Geomar Pier in Kiel. At this time, two more talks by students were given.

5 Participants

Table 1: List of scientific crew.

Name	Position	Institute
Prof. Dr. Christian Berndt (09/06/2019 - 09/10/2019)	Chief Scientist	GEOMAR
Prof. Dr. Sebastian Krastel (09/10/2019 - 09/14/2019)	Chief Scientist	University of Kiel
Dr. Jens Schneider v. D. (09/06/2019 - 09/10/2019)	Senior Scientist	University of Kiel
Kai Frederik Lenz	Senior Scientist	University of Kiel
Dr. Philipp Held (09/10/2019 - 09/14/2019)	Senior Scientist	University of Kiel
Per Oscar Nilsson (09/10/2019 - 09/14/2019)	Master Student	University of Stockholm
Michael Kühn (09/06/2019 - 09/10/2019)	Master Student	GEOMAR/University of Kiel
Anna Christina Hans	Bachelor Student	University of Kiel
Tatjana Michaela Weiler	Bachelor Student	University of Kiel
Jonas Liebsch	Bachelor Student	University of Kiel
Theresa Prigan	Bachelor Student	University of Kiel
Tilman May	Bachelor Student	University of Kiel
Johanna Klein	Bachelor Student	University of Kiel
Kelvin Rathiens	Bachelor Student	University of Kiel
Pascal Koch	Bachelor Student	University of Kiel

Table 2: List of crew from Reederei Briese.

Name	Position
Helge Volland	Master
Christian Gräber	1st Officer
Sebastian Neugebauer	2nd Officer
Hans Jörg Freund	Chief Engineer
Matthias Jensen	Electrician
Hardy Schwieger	Boatswain
Ken Schnieders	A.B.
Benjamin Brüdigam	A.B.
Lucien Delachaux Dit-Gay	A.B
Willi Rieger	A.B.
Thomas Kirschnick	Cook

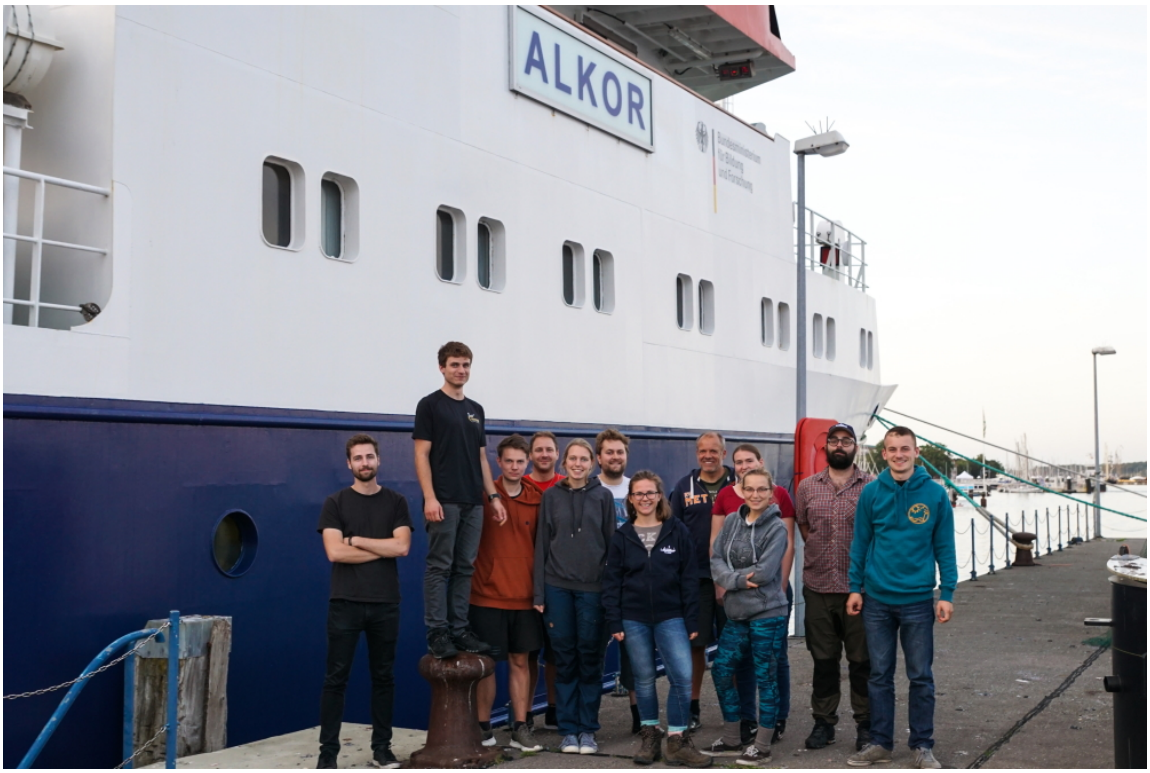

Figure 3: Group picture of the scientific crew of AL527.

6 Methodology

6.1 2D reflection seismic

A Sercel Mini GI-Gun was used as seismic source during the seismic surveys. The chamber volume of the Mini GI-Gun was reduced by Micro Shuttles to 0.1 l for the generator and 0.1 l for the injector. Most of the time the airgun was operated with 120 bar gun pressure and an injector delay of 18 ms. The shooting interval varied between 7 s and 10 s with a vessel speed around 4.5 kn. That leads to a shooting-point distance of 2 m to 2.8 m. We estimated a signal delay of 21 ms. The Streamer used in the surveys contained 6 sections with 8 channels per section and a group spacing of 1.56 m and a total streamer length of 75 m. We used a 24.5 m stretch in front of the streamer. Exact information about the geometry is visualised in Figure 4. We did not use birds for the streamer as it was comparably short, but we fixed floats to the Analog-to-digital (AD) converter instead. For that reason, we were limited in controlling the depth of the streamer. Each streamer section had an analog digital converter. The communication between the AD-converter modules and the recording system was transmitted via TCP/IP protocol. A repeater was located between the deck cable and the tow cable. The power supply as well as the communication with the AD-converter was managed by the power supply unit.

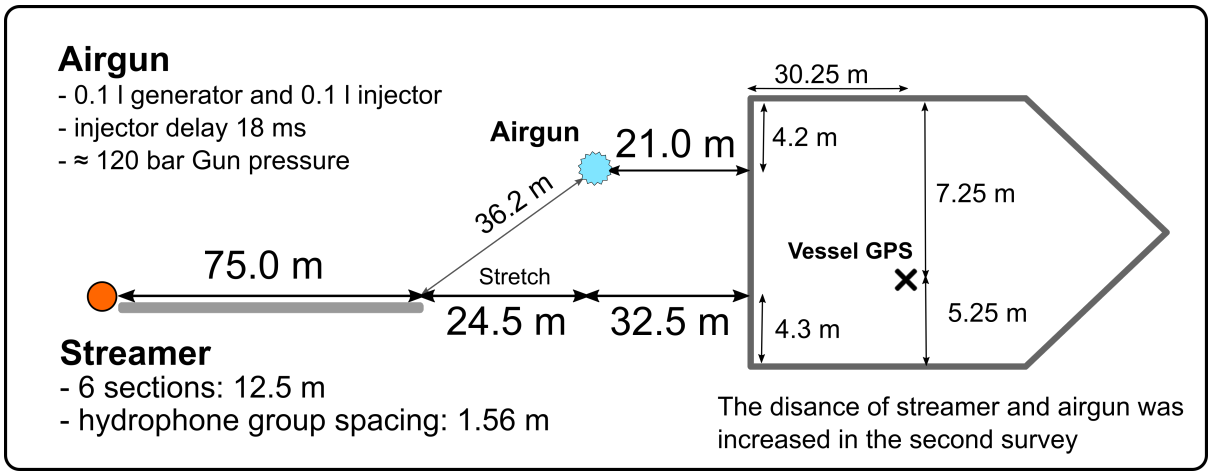

Figure 4: Deck geometries, streamer configuration and gun setting for the 2D reflection seismic surveys.

The reflected seismic signal was sampled with 500 μs and an overall length of 3 s for every shot. The seismic data was recorded as multiplexed SEG-D where seperate files were generated for every shot. The acquisition computer allowed a live quality control. We used the GPS system of the R/V Alkor to log time as well as position and speed of the vessel. Unfortunately, there were some interruptions of the GPS system within line 202 which should be considered when using this data.

6.2 NORBIT Multibeam

Upon arrival on the vessel, we installed a NORBIT STX prototype Wideband Multibeam System (MBES) in the moonpool. The STX prototypes integrates an Applanix Wavemaster motion and inertial navigation system (IMU), which corresponds to a sound velocity probe next to the sonar head. A dual GPS antenna was installed at the rail of ALKOR's top deck and connected to the IMU. Installation offsets on ALKOR were taken from previous installation (Table 3). We supplied RTK corrections (15-AXIO-NET) via the on-board internet to support the dual antenna GPS recordings.
The NORBIT MBES produces a chirp signal with a 500 μs lasting pulse resulting in 80 kHz bandwidth. 512 beams are formed with a beam resolution of 0.9° across-track and 0.9° resolution along-track at 400 kHz. Range resolution can achieve accuracy of up to 1 centimeter in shallow water. We sailed our surveys with 140° to 150°. The opening angle was variable depending on the bathymetry characteristics. Attitude data (.000 format) was collected with 200 Hz to allow for later post-processing of the IMU data. QINSy 8.18.3 and the NORBIT GUI recorded .db and .s7k data in parallel for bathymetry, backscatter, and snippet backscatter. MBSystem and QPS Qimera were applied for post-processing. The strength of backscatter values is influenced by a number of characteristics: the strongest impact to intensity comes from the distance of the reflecting surface to the MBES radiator, and the angle in which the beams impinge the seafloor (Figure 5B). During processing both of those effects are mostly removed from the backscatter grid, leaving behind mostly backscatter effects of the surface which result from differences in sediment grain-size, micro-topography, biology and moisture of the topmost layer (Figure 5C-F). For assessing vertical profiles of sound velocity we used a multisensor Conductivity, Temperature, Depth (CTD) profiler 75M manufactured by Sea & Sun Technology. It is a self-sustaining probe, which is powered by batteries and can operate up to a depth of 1000 m. Three of the eight channels were equipped with a pressure, conductivity, and temperature sensor. Furthermore, the time mode was used to record UTC stamps with a sampling rate of 0.1 s. From the data, we derived the salinity, sound velocity, density, and acoustic absorption values.

Table 3: Installation lever arm offsets between the POSMV Wavemaster primary antenna mounting point and the sonar head flange.

Applanix coordinates	**Offset [m] to primary antenna on the top deck**
X	3.92
Y	3.82
Z	-15.73

After approximately one hour of sailing the IMU completed its self-calibration. The IMU also achieved fix RTK GPS leading to accuracies up to 5 cm for position and height

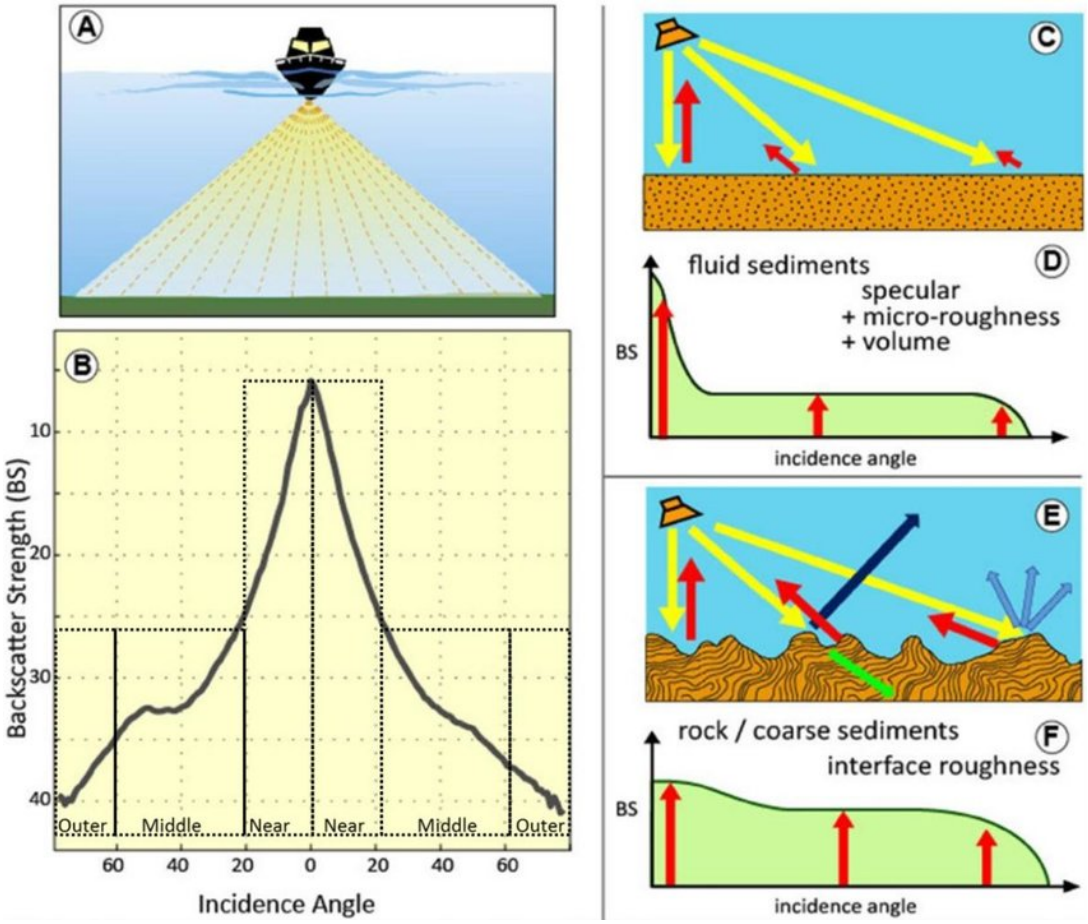

Figure 5: Influences to backscatter signal strength taken from Lurton & Lamarche (2015)

Table 4: Parameter Setup before and after the calibration (reference to COG was not provided).

Parameter	Initial GAMS value	Final GAMS value
Baseline Vector X	0	0.085
Baseline Vector Y	2	1.998
Baseline Vector Z	0	-0.001

most of the survey time. The roll calibration was conducted during a mattress survey in the Bay of Mecklenburg close to the coast of Brook. Bottom detection was reliable within the 140° sector, deteriorated with noise at 150°. Simultaneous recording of bathymetry, sidescan, snippet sidescan and water column was feasible at slow survey speed. Bathymetric data were recorded at survey speed between 3 kn to 5 kn and ping rates between 5 Hz to 10 Hz. Heave might be improved by post-proccessing (true heave) or RTK heave application.

6.3 INNOMAR Sediment echosounder

We used a parametric subbottom profiler of type Innomar SES-2000® medium which is hull-mounted on the R/V ALKOR. It transmits two high frequencies at high sound pressure. These two sound waves interact in the water column, generating harmonics. The SES-2000® medium sends and records primary frequencies of about 100 kHz and thus generates parametric secondary frequencies within the range of 4 kHz to 15 kHz. Secondary frequencies develop through nonlinear acoustic interaction of the primary waves at high signal amplitudes. The advantage of these secondary frequencies is the fact that they have a similar beam width and short pulse lengths as the primary frequencies despite the low frequency and the small transducer. The system allows a simultaneous acquisition of up to three different frequencies (multi-frequency mode), which are shot sequentially. Every shot is recorded by two channels, comprising a primary high frequency (HF) and secondary low frequency (LF) as full waveform and envelope. The secondary frequencies are adjustable and were set to 4 kHz with two pulses and to 15 kHz with one pulse during all surveys. The system has a vertical resolution of 6 cm and its accuracy depends on the frequency and water depth, e.g. 100/10 kHz: 2/4 cm + 0.02 % of the water depth. The soundings are corrected for heave, roll and pitch movements of the vessel. The system worked reliable and produced high-quality data throughout the whole time. After recording, the full waveform data was converted into the segy-format with SES-convert (version 2.3.0.2). If seismic data was collected simultaneously, one SEG-Y file was created for the length of each seismic profile. We imported the converted segy-files into IHS Kingdom seismic interpretation software and calculated the envelope subsequently.

6.4 EK60 fishery echosounder

The ship-board fishery echosounder KONGSBERG EK60 was operated with a frequency of 120 kHz for detection of gas bubbles. The data were not processed during the cruise and just recorded for a potential further use.

6.5 Gravity core and grabber sediment sampling

A gravity corer was used for taking sediment samples. It uses a 800 kg weight to press a 5 m long metal pipe into the ground. In order to collect and secure the core afterwards, a plastic pipe was installed within the metal pipe. Further, we used a core catcher at the end of the pipe to prevent sediments from falling out of the pipe. With this setup we were able to collect cores with up to 4 m length. Once the samples were taken, the plastic pipe was cut in 1 m pieces for closer investigations and archiving.A simple grab was used to get samples of the surface of the seafloor. The findings were documented

by pictures and small quantities were secured. The individual positions for gravity coring and grabbing are shown in Figure 6.
The SES data was used to choose interesting grab points considering topographical characteristics. The limited maneuverability of the vessel and the influence of water current makes it impossible to determine a grabbing point down to single meters. This influenced the choice-making of the grab points, some were intentionally chosen to be in areas of constant backscatter, while some were chosen in areas of the backscatter changing in small dimensions, to get a chance to collect information about some darker spots. These could show larger rocks, or biological features on the seafloor.

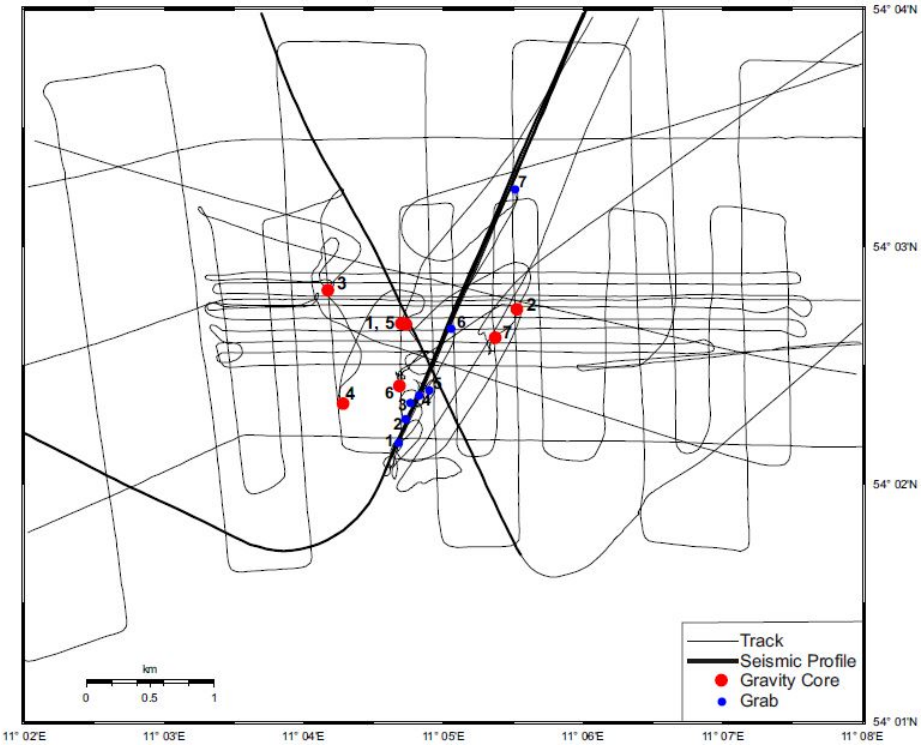

Figure 6: Positions of graps and gravity cores taken in the Bay of Mecklenburg.

Figure 7: Deployment of a gravity corer (left) and example of a grab (right).

6.6 Video Camera

We conducted underwater filming in order to search for the missing observatory. For that purpose, we used a Mariscope-UW-Video-camera. The camera was lowered on the side of the vessel until the seafloor got into view. The depth of the camera was adjusted permanently as the ship moved. Unfortunately, the weak lights of the camera made it impossible to film in regions deeper than approx. 20 m. Further, the size of the image was small compared to the research area. Thus, it was hard to cover the area systematically for limited moving options and the low visual range. The camera was supplied by a power supply unit. The data was observed and recorded live on a connected computer.

7 Preliminary Results

7.1 Identification of sediment and biological characteristics

To get a better understanding of the composition of sediments and biological features at the seafloor of the Bay of Mecklenburg the same track has been surveyed twice, first using the Multibeam Echosounder (MBES), and then using the INNOMAR Sediment Echo Sounder (SES). Darker areas in the resulting backscatter grid show areas of stronger backscatter, and brighter values show areas of weaker backscatter (Figure 8).

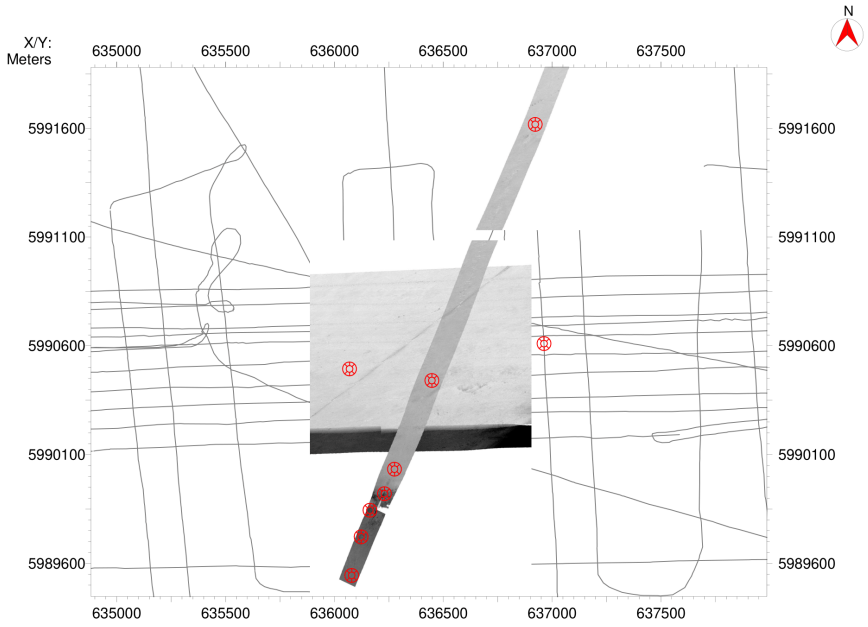

Figure 8: Complete backscatter data survey including chosen grab points, 1 in SW, 7 in NE ends of survey.

The first grab point was chosen in an area of evenly colored backscatter in with a dark gray tint. The SES data shows that this point is located on an underwater hill, with an elevation of around 2 m above the valley in the north east (Figure 9, grab_01). From prior exploration of the area it is clear that this hill is a sunken beach. The sediments that were expected to be found were mostly moist sand, without larger rocks or vegetation. The sediments that were excavated showed the expected characteristics: smooth, sandy silt, with weak to no odor, and small sea shells, without larger rocks.
The second grab point was chosen to be in an area of backscatter with equal overall intensity, but containing smaller, rock-sized areas of higher backscatter values. Hence, the expected sediments were similar to the ones excavated from the first grab. But,

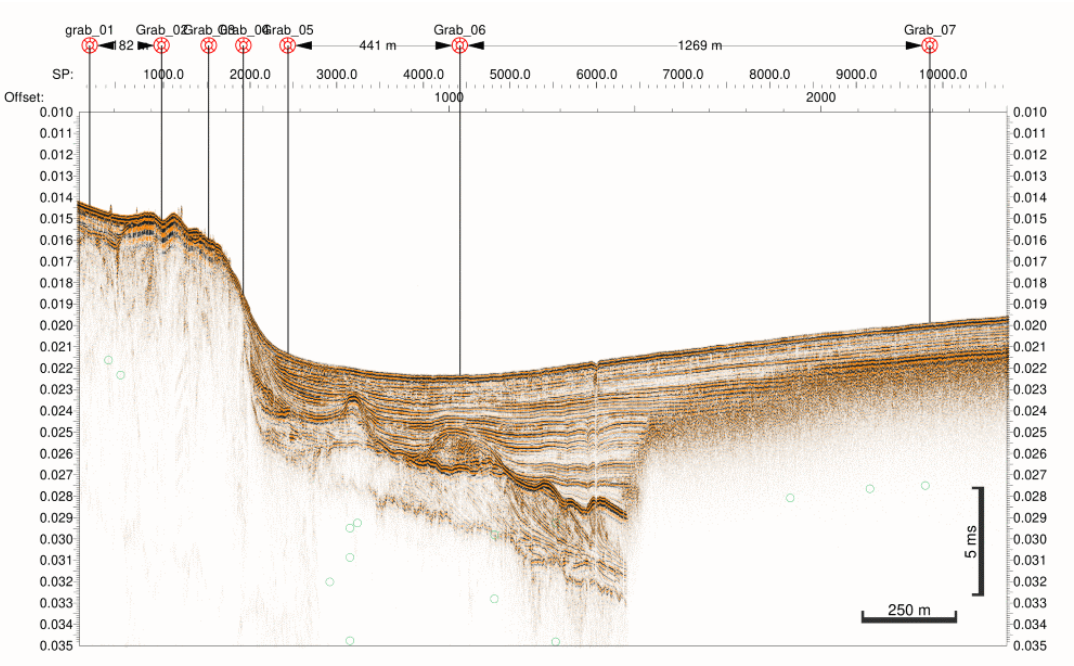

Figure 9: Complete SES data survey including chosen grab points.

considering the low precision of the ship and grabber placement, it could either hit a brighter or darker spot, the former being very similar to grab 1, and the latter containing larger rocks, or underwater plants. This was the case, the sample was largely similar to grab 1, but it contained less sea shells, and more, larger rocks with diameters up to 2 cm.

The third grab was the first one that was collected on the slope down from the beach leading to the valley (Figure 9, Grab_03), and lies in an area characterized by even darker patches of backscatter. Continuing the trend, it was expected to contain even larger rocks. And indeed the excavation results contained a large rock with a diameter of 15 cm, within mostly sandy, silty and badly sorted mud. It also contained smaller flint stones and rocks with sharper edges, these have likely rolled down from the beach in more recent times. There were only a handful of small sea shell pieces scattered within the sediment.

Grab 4 was chosen to be in another area of strong, dotted backscatter on a slowly brightening background. It is located on the steepest point of the hillside (**??**) and was believed to contain more sediments that fell down, and similarly sized rocks as the ones that have been found in grab 3. The examined sediment sample had a faint smell, and didn't contain large rocks, sea shells and was made mostly out of a mix of very small rocks, mud and sand. These findings lead to the conclusion that the grab was probably executed in a spot with brighter backscatter, and not at one of the darker spots.

The fifth grab sample was collected at the foot of the slope (Figure 9, Grab_05), in an area of evenly colored, light gray backscatter. The sediments found in the valley were

expected to be quite similar, with the amount of rocks and sea shells decreasing with increasing distance to the beach.
The findings were matching the expectations well, grab 5 contained small rocks (diameter of 2-3 cm), and small pieces of sea shells, and had a strong odor. Grab 6 contained very fine, silty sediment, and very small rocks (diameter of 1-5 mm). No sea shells were found in this sample, which corresponds to the long distance of about 500m between the location of the beach and grab 6.
The last grab point, grab 7, was collected at the end of the survey, at a distance of about 1.5 km from the beach, on a slow upwards slope (Figure 9, Grab_07), and at one of the brightest areas of backscatter along the survey track. As was the case with grabs 5 and 6, this sample also had a strong odor, and was very well sorted, with no rocks, sea shells or sand among the silty clay this sample was made of.
In conclusion the preliminary results of the survey show that judging from a combination of MBES backscatter and SES data the composition of sediments and biological traces at the seafloor can be predicted very well. Sediment samples collected via excavating with a grabber were largely consistent with the expectations.

7.2 Fate of the seafloor observatory at Boknis Eck

The COSYNA node system at Boknis Eck consisted of a shore-side container with power supply and server, as well as a shore connection cable, a sea-side node, data cable and two measuring stations. The first station was known as the Underwater Observatory and the second one as the Coastsens Tower (Helmholtz-Zentrum, n.d.). On 21st of August, 2019 the node (dimensions LxWxH: 2.4 x 1.4 x 1.2 m) and the observatory (dimensions LxWxH: 1.2 x 1.2 x 1.2 m) went missing.
A 3D bathymetry map generated by Qimera was used then to determine coordinates of conspicuous points in the area close to Boknis Eck. At these positions underwater filming was done later on. The evaluation of the backscatter profiles showed that the tower and the weights are still in the correct position. This could be confirmed with the underwater video camera. Two conspicuous points in the vicinity (70 m away) of the tower turned out to be railway wheels. Two further conspicuous points could not be identified by the camera. A particularly conspicuous drag mark with a length of 400 m, a width of 2 m and a depth of on average 20 cm passed the tower at a distance of about 200 m. At the end of the grinding track, an atypical elevation was visible, which could be very well represented by backscatter intensity. Since this elevation is a rectangular object of approx. 1.4 m x 1.2 m in size, it was obvious to assume that it was one of the missing devices. See also Figure 10. In summary it can be said that it was not possible to detect the missing devices. However, the surrounding area could be mapped. Coordinates of suspicious positions are passed forward to Geomar for further

investigations.

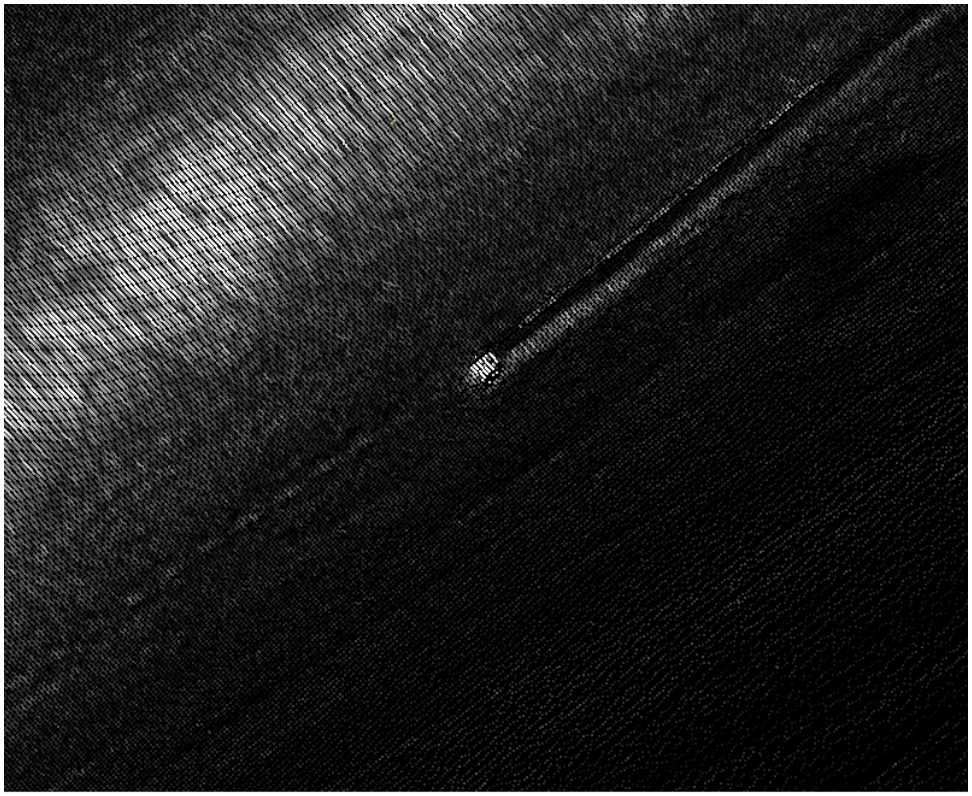

Figure 10: Object at the end of the conspicuous grinding track as derived by backscatter data by NORBIT MBES.

7.3 Spatial expansion and geological structure of a former beach in the Bay of Lübeck

The data were obtained with Innomar using a frequency of 8 kHz close to the Bay of Lübeck, processed and interpreted with IHS Kingdom Suite. In the Bay of Lübeck a former beach was expected, which was covered by sediments because of a rise in sea level when the present Baltic Sea was formed.

Since the focus of this exploration was the former beach, it will mainly be focused on the grid of the top of the sand, which is presented in Figure 11. Beginning with the dimensions, it has to be said that there are large gas accumulations (approx. 4 %) in the northern part of the survey. These accumulations make it impossible to get any valid data from this area. Therefore, the beach could possibly continue further north than presented in the data. In order to make a clear statement about that, different methods than the SES are necessary. In the south of the survey, a slope appears on the seafloor. This slope pretty much marks the southern boundary of the former beach, where the top part of the beach is just 19 m below the sea surface. The bottom of the

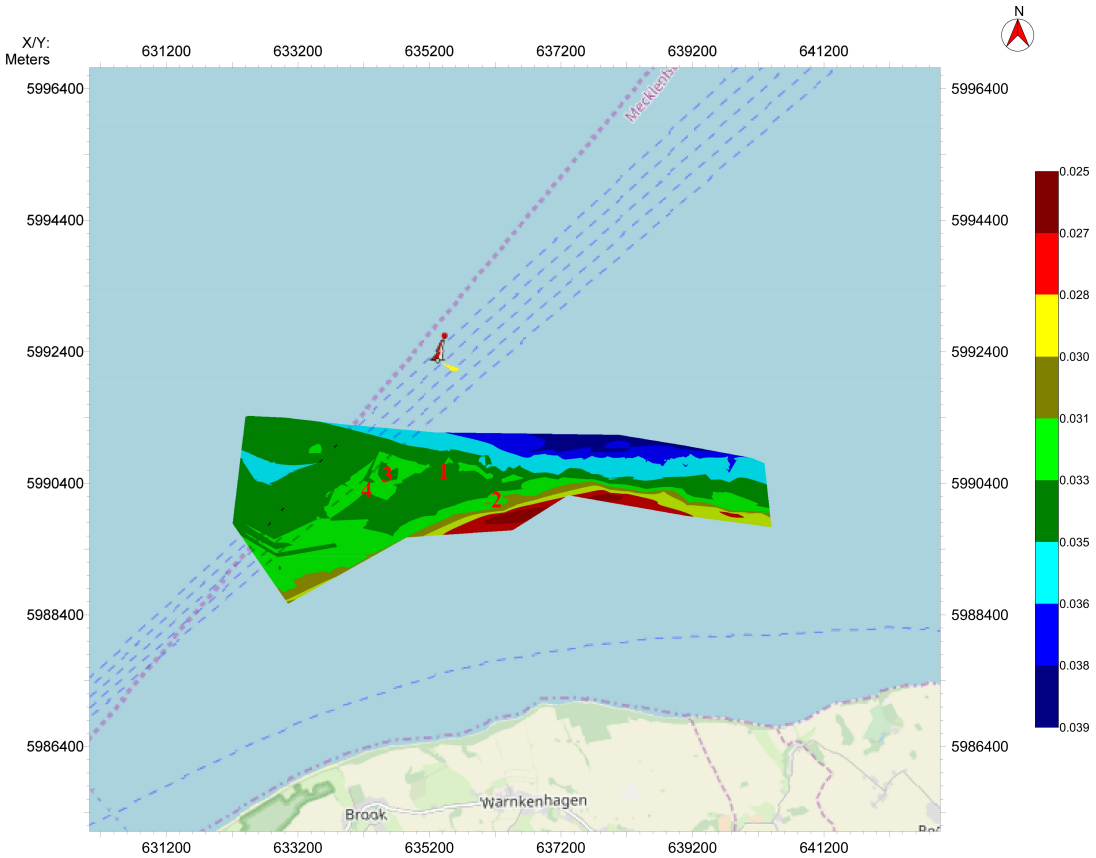

Figure 11: Top of the former beach in the Bay of Lübeck as conduted from SES data visualized with Kingdom Suite.

sand occurrences is harder to recognize, since the signal strength is getting significantly weaker proportional to the depth. The most distinct features in the collected data are two sandbanks, which are located in the very middle of the survey. Both of them are orientated in east-west direction, and thus along the general beach trend, and can be found between 23 m to 26 m below the sea surface. One of the sandbanks (point 2 in Figure 11) is located close to the southern boundary of the beach. Since we only collected 2D data, the algorithm did not calculate a continuous line for the sandbank. Nevertheless, the presence of a sandbank is supported by the signals to its right and left, even though the signals are weaker than the ones of the other sandbank. The second sandbank starts pretty much in the north of the first one. This leads to the assumption that both sandbanks could have the same origin. But, either way, starting from that region, the sandbank extends towards the north-west. At point 1, the sandbank seems to be disrupted as a line is going exactly through it. However, considering the other lines, it is more likely that the structure bends towards the north, forming some kind of arc around point 1. Further west, there is a small basin (point 3), which can be seen in the vertical and horizontal lines. Right next to it, there is another small interruption (point 4). The appearance of this interruption is not as smooth and natural as the one of the basins in point 3, since it originated from seafloor subsidence due to gas leakage.

In general, it was very hard to gather any meaningful information about the bottom of the sand structures, since they were not easy to pick and partly not visible due to the presence of gas especially in the northern part. Nevertheless, the grid shows a general trend from south to north with the southern part being closer to the surface. In the very north, the bottom of the sand structures reaches a depth of 33 m. Considering the lines, it can be assumed that they even reach further down. On the basis of SES data alone, no indication can be given about this thesis due to the increased gas content in the northern area. Apart from analysing the layers individually, I calculated the thickness of the beach by subtracting the grids for the top and the bottom of the sand structures. In the resulting grid, it can be seen that the thickness is at its maximum with about 9 m at the position where the sandbanks are supposed to be. Other than that, there is a general trend with increasing thickness of the beach from south to north. In the eastern part of the considered area, the sand accumulation is very thin ($<$1 m). This can be a true effect but it also might just be the result of insufficient data in the lower parts of the ground, where the bottom of the beach was quite hard to find.

7.4 Acoustic characterisation of gas

Gas fields beneath the seafloor emerge when biological material dies off. Methanogens, microorganisms which are common in anaerobic surroundings, are responsible for this gas formation as they produce methane out of carbon dioxide (Balch *et al.* , 1979). If the formed gas is covered by a sufficient thick layer of silt, the gas will not be able to escape but remains as a silt layer enriched with gas. Such gas fields can be observed in the Bay of Mecklenburg.

To study the acoustic characterisation of gas, hydroacoustic surveys at different frequencies along the same profile line were compared. In this case, data from the Innomar Sediment Echosounder (SES) at 4 kHz, 5 kHz, 6 kHz, 8 kHz, 10 kHz, 12 kHz and 15 kHz as well as seismic data at a frequency of about 300 Hz were analyzed. The considered profile line is situated in the Bay of Lübeck close to the coast of Brook and has an east-west orientation. The boundary points are located at 54°02'17.37" N, 11°04'46.51" E and at 54°03'01.26" N, 11°05'17.45" E and thus cover a distance of 1.5 km. According to the 4 kHz SES profile presented in Figure 12, the observed seafloor is characterized by a more highly situated area in the west. The water depth in the remaining profile is about 5 m lower. At an offset of 1400 m, a vertical disturbance is visible as a vertical blank. At the eastern edge of the profile, a gas layer is visible at 2 m depth. In general, an emitted acoustic signal is scattered by the gas layer, so that the backscattering of gas is more diffuse compared to the backscattering of the layered silt. Further, the acoustic energy is completely absorbed by the gas layer, so that the acoustic signal

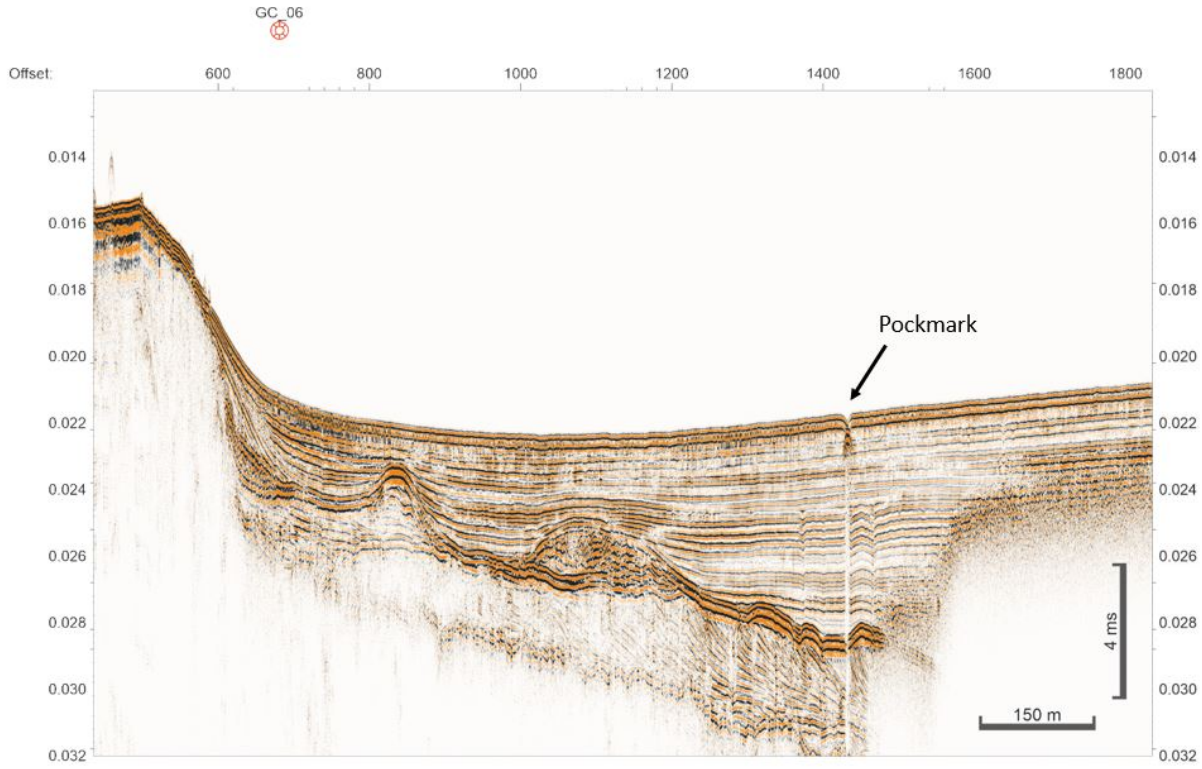

Figure 12: West-east orientated Innomar SES profile at 4 kHz close to the coast of Brook, extending from 54°02'17.37" N, 11°04'46.51" E to 54°03'01.26" N, 11°05'17.45" E.

cannot reach further down. According to these two effects, gas can be identified in SES data by acoustic turbidity and acoustic blanking (Sunjay, 2011).

The usage of different frequencies for the SES leads predominantely to different vertical resolution, in this case to 10 cm for the 15 kHz and to 40 cm for the 4 kHz survey.Thus, the layers of the seafloor are represented more detailed the higher the resolution is, as can be seen in Figure 13. However, considering the representation of the mentioned vertical disturbance as well as the transition zone to the gas enriched layer, this relation does not apply. Instead, the seafloor is represented best in the 10 kHz survey as blanking is minimized at that frequency (Figure 13).

The gas layer is also visible in the seismic survey presented in Figure 14. It is visible because of a phase inversion of the reflectors at the eastern end of the survey. This phase inversion arises as the acoustic impedance decreases from water to gas while it increases from water to soil. Further, gas is a stronger reflector than soil which explains the greater number of clearly visible multiples at the eastern side of the survey. The transition area is still characterised by a phase inversion. Nevertheless, the multiples are not as distinct as in gas layer, which can be explained by the difference in total gas content.

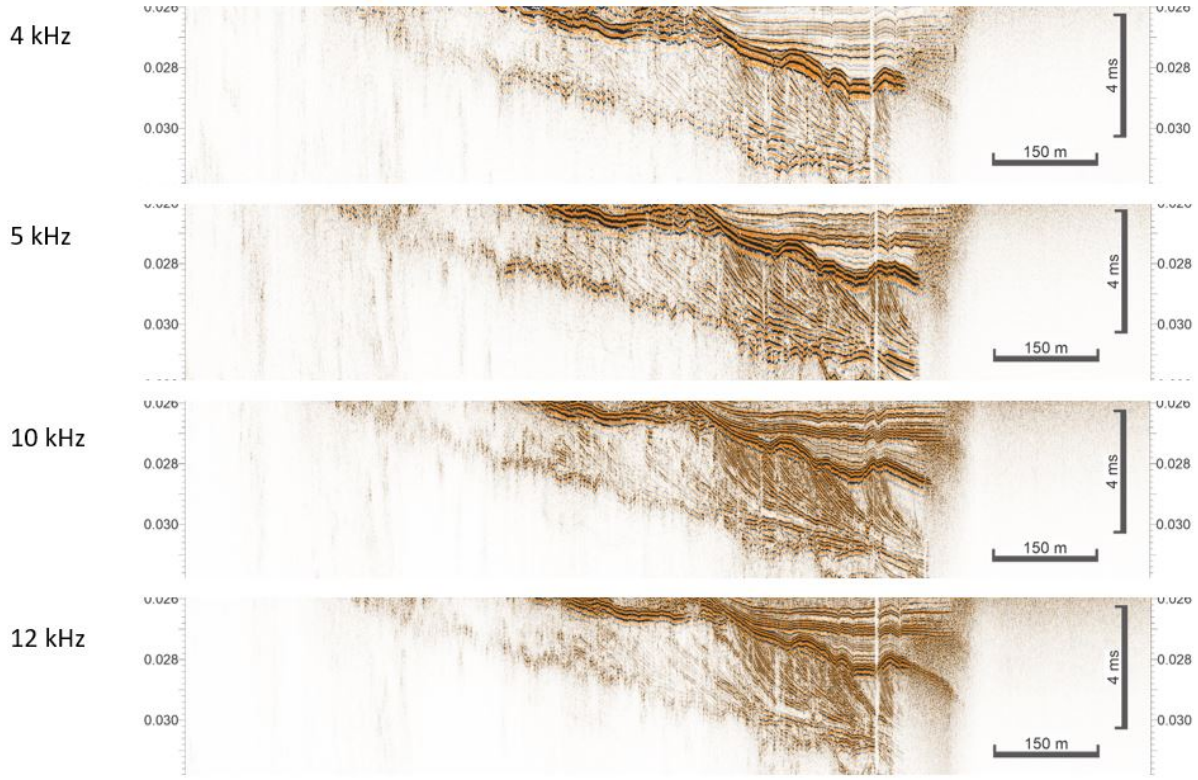

Figure 13: West-east orientated Innomar SES profile at different frequencies cut off between 26 ms and 32 ms.

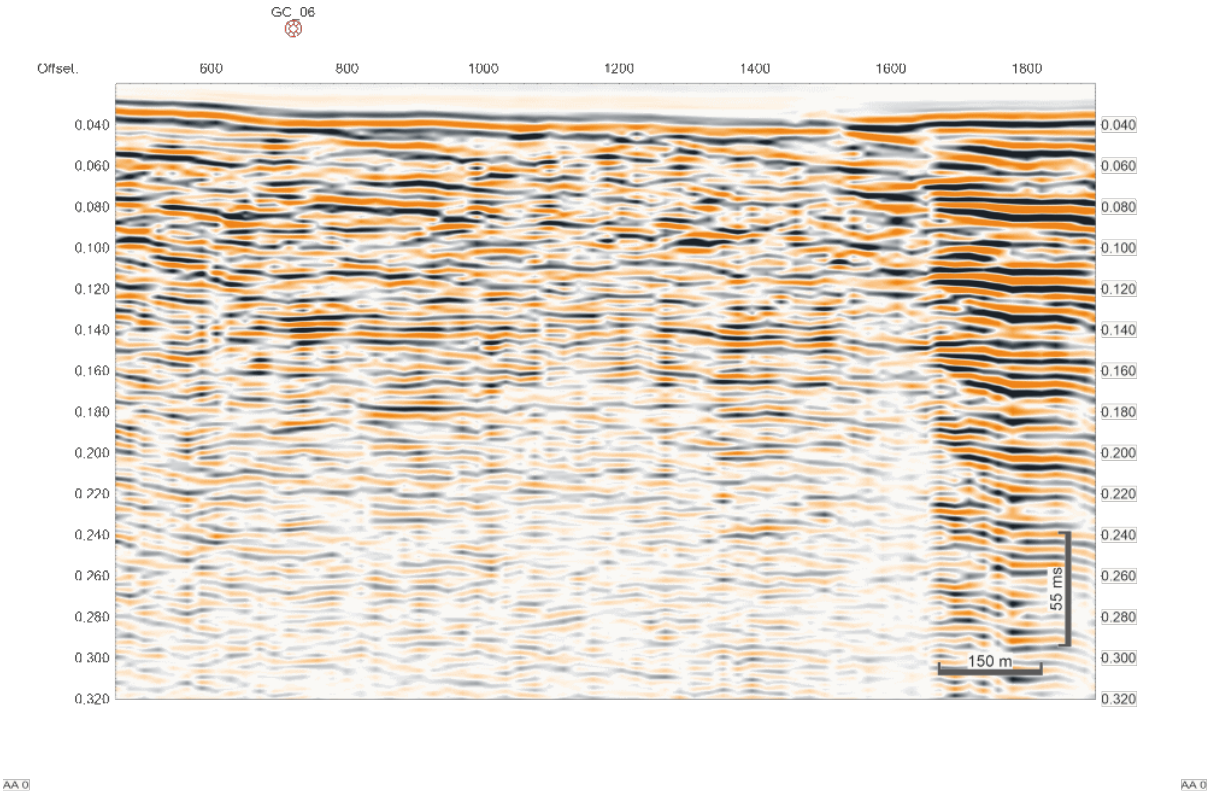

Figure 14: West-east orientated seismic profile.

7.5 Tectonic structures in the Bay of Mecklenburg

The profiles P202 (Figure 15) and P205 (Figure 16) both show some interesting geological structures. Profile P202 starts in the west of the Fehmarn Belt and ends in the east. The seafloor is located at 0.033 s TWT, the first and second multiple are located at 0.066 s TWT and 0.099 s TWT. The profile P205 starts east of the Fehmarn Sund and is running towards Travemünde. As the seafloor in P205 is located at 0.025 s TWT, the first and second multiple of the seafloor are located at 0.05 s TWT and 0.075 s TWT. In Figure 15 an anticline and syncline structure is clearly visible over the whole profile. There are also some zones of seismic blanking marked in Figure 15 between 13 km and 20 km. Seismic blanking is an indicator for the occurrence of gases in the ground. At the beginning of profile P205 the seafloor reflection shows a reversed seismic polarity which indicates high gas content in the pore space. There is also an anticline visible in Figure 16 at about 34 km offset and it's first visible at about 0.15 s TWT.
The 2D seismic data in the Bay of Mecklenburg is characterized by a lot of the recognized anticline and syncline structures. It can be explained by halotectonics. There must have been a time when the salt, which deposited probably in the Zechstein, moved upwards due to its lower density. So the overlaying deposited sediments started to be bent upwards by rising saltpillows.

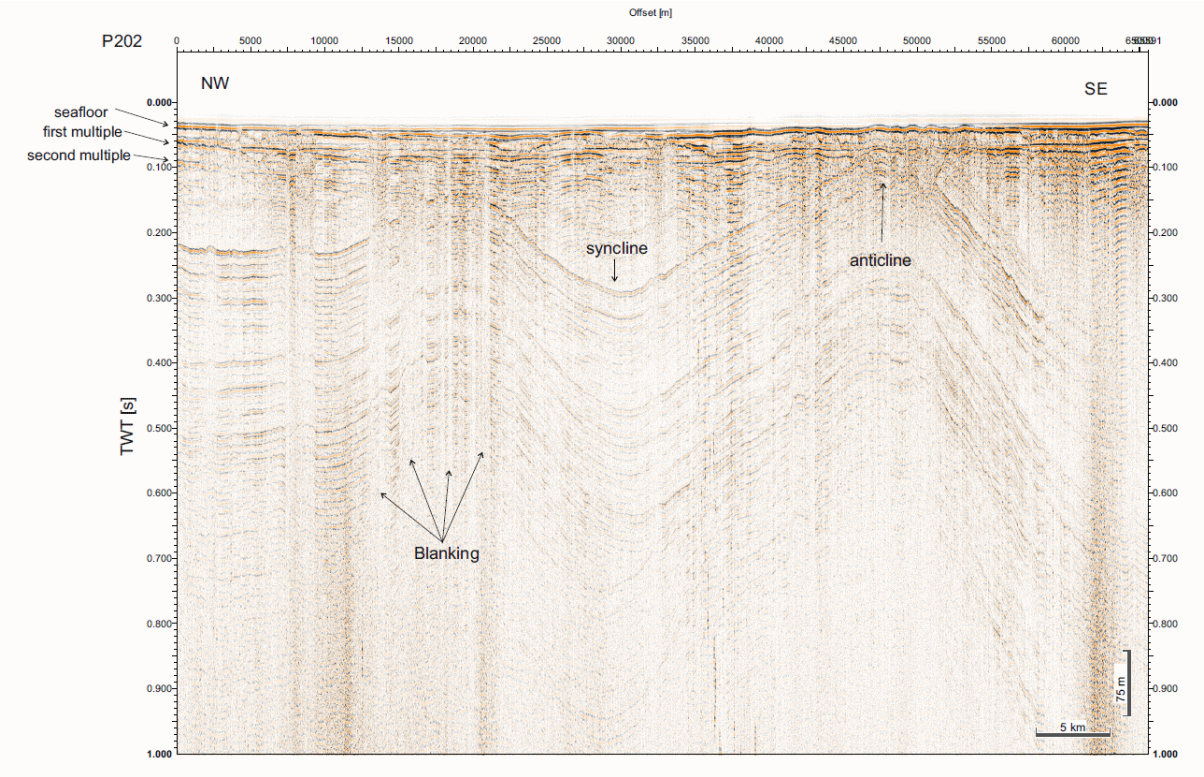

Figure 15: Seismic Profile P202 crossing the Fehmarn Belt from west to east.

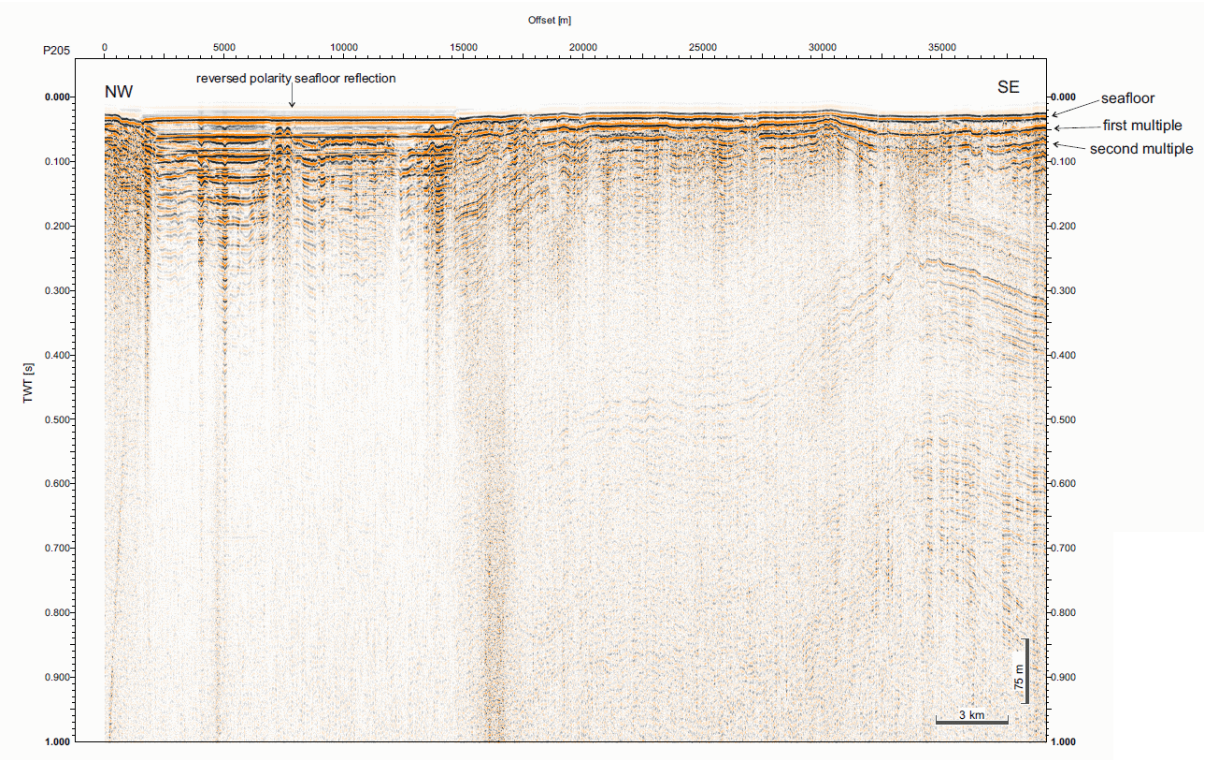

Figure 16: Seismic Profile P205 starting near the Fehmarn Sund und running in south-west direction.

8 References

Balch, W. E., Magrum, L. J., Fox, G. E., & Woese, C. R. 1979. Methanogens: A Re-evaluation of a unique biological group. *Microbiological reviews*, **43**(2), 260–296.

Baschek, B., Schroeder, F., & Brix, H. 2017. The Coastal Observing System for Northern and Artic Seas. *Ocean science*.

Berndt, C. 2005. Focused fluid flow in passive continental margins. *Philosophical transactions of the royal society a: Mathematical, physical and engineering sciences*, 2855–2871.

Berndt, C., & Karstens, J. 2019. Cruise Proposal for the project ACT-SENSE: Bodenmessungsbasierte Überwachung der Integrität von CO2-Speicherstätten.

Forschungstaucher, Uni Kiel/DPA. 2019. *https://www.spiegel.de/wissenschaft/natur/bild-1285237-1465827.html (last access: 16.09.2019)*.

Heinrich, C., Schwarzer, K., & Feldens, P. 2016. Submerged beach ridges in Mecklenburg Bay (SW Baltic Sea) indicate Late-Pleistocene and Holocene shore lines. *In: 35th International Geological Congress, Cape Town, South Africa*.

Helmholtz-Zentrum, Geesthacht. *COSYNA Unterwasserknoten-System, https://www.hzg.de/institutes_platforms/cosyna/observations/underwater_node/index.php.de (last access: 16.09.2019)*.

Hübscher, C. 2010. Structure and evolution of the Northeastern German Basin and its transition onto the Baltic Shield. *Marine and petroleum geology*.

Karstens, J. 2018. Cruise Report R/V ALKOR 512: North Sea Blowouts, Cuxhaven - Kiel (Germany) 15.07. - 26.07.2018. *GEOMAR report*.

Lurton, X., & Lamarche, Geoffroy. 2015. Backscatter measurements by seafloor-mapping sonars.

Römer, J. 2019. 800 Kilo Messstation von Meeresgrund verschwunden (04.09.2019). *Spiegel online*.

Sunjay, S. 2011. Geophysical prospecting of gas hydrate. *Pages 79–83 of: Technical and geoinformational systems in mining*. CRC Press.

Winterhalter, B. 1992. Late-Quaternary stratigraphy of Baltic Sea basins - a review. *Bulletin of the Geological Society of Finland*, **64**(2), 189–194.

9 Acknowledgements

We would like to thank Captain Helge Volland and the entire crew of R/V ALKOR for their excellent support and hospitality during the entire cruise. Speaking for all students, we thoroughly enjoyed this cruise, learning about marine geophysical methods and processes and generally feeling very well instructed. We would like to thank all of the scientific and the on-board crew for making this cruise a great experience for all of us.

10 Acquisition protocols

Time	Latitude	Longitude	Course [°]	Heading [°]	Speed O.G. [kn]	Depth [m]	Source	Shot interv. [s]	Rec. length [s]	Leakage	FFN	Injector Delay [ms]	Gun-Pressure [bar]	Remarks
UTC	xx° xx.xxx‘	xx° xx.xxx‘												
Friday, 06.09.2019														
Seismic Survey S100														
17:40	54° 31.531	010° 02.401	291	282	3,5	28	Micro GI	7	3	21,0	1000	20,0	120	6 sections in water. Survey al527-3. first file number is 1000. ch 33 dead. Sampling frequency 0.5ms
17:54	54° 32.199	010° 03.117	86	97	3,8	26	Micro GI	7	3	25,0	1130	20,0		SOL P101
18:00	54° 32.168	010° 03.788	91	97	4,4	26	Micro GI	7	3	26,0	1183	20,0	80	
18:20	54° 32.123	010° 06.020	92	94	4,1	22	Micro GI	10	3	28,0	1336	20,0	45	changed shot interval to 10s due to low pressure
18:28	54°32.116	010° 06.998	90	94	4,2	22	Micro GI	10	3	28,0	1380	20,0		checking on dropping pressure, no info within shot window. Shots 1377-1436:empty shots
18:36	54° 32. 111	010° 08.140	93	115	2,2	22	Micro GI	0	0	28,0	1436	20,0		turning trigger off, taking gun in
18:58	54° 32.089	010° 09.419	95	126	1,8	22	Micro GI	0	0			20,0		finished taking streamer and shotgun in
Saturday, 07.09.2019														
Seismic Survey S200														
12:57	54° 32.360	010° 43.980	72	69	4,6	22	Micro GI	10	3	19,0	2000	20,0	120	6 sections in water. Survey al527-4. first file number is 2000. Sampling frequency 0.5ms
13:00	54° 32.481	010° 44.555	70	67	4,6	22	Micro GI	7	3	20,0	2015	20,0	120	
13:06							Micro GI	7	3		2068			Sol 201
13:07							Micro GI	7	3		2074			only generator for testing
							Micro GI	7	3		2087			only injector for testing
							Micro GI	7	3		2113	0,0		injector and generator 0 ms delay
							Micro GI	7	3		2141	20,0		testing delays
							Micro GI	7	3		2150	18,0		testing delays
							Micro GI	7	3		2159	16,0		testing delays
13:18							Micro GI	7	3		2164	18,0		testing delays
13:22	54° 33.126	010° 47.358	67	63	4,5	23	Micro GI	7	3	27,0	2210	18,0	120	
13:45	54° 33.780	010° 49.994	67	61	4,4	21	Micro GI	7	3	29,0	2401	18,0	122	
14:05	54° 34.402	010° 52.570	67	61	4,5	16	Micro GI	7	3	29,0	2577	18,0	120	
14:25	54° 34.963	010° 54.790	69	65	4,6	16	Micro GI	7	3	30,0	2743	18,0	120	
14:45	54° 35.598	010° 57.358	67	71	4,7	21	Micro GI	7	3	30,0	2922	18,0	122	
15:05	54° 36.130	010° 59.699	68	72	4,5	36	Micro GI	7	3	30,0	3090	18,0	123	
15:25	54° 36.661	011° 01.818	67	75	4,8	22	Micro GI	7	3	30,0	3250	18,0	122	
15:45	54° 37.394	011° 04.828	68	77	4,8	24	Micro GI	7	3	31,0	3440	18,0	122	
15:49	54° 37.508	011° 05.288	71	85	4,6	24	Micro GI	7	3	31,0	3469	18,0	122	EOL 201 SOL 202
16:05	54° 37.003	011° 06.949	130	131	4,6	26	Micro GI	7	3	31,0	3605	18,0	123	
16:25	54° 36.079	011° 09.049	126	128	4,5	28	Micro GI	7	3	31,0	3778	18,0	123	
16:38							Micro GI	7	3		3689	18,0		GPS Aussetzer
16:45	54° 35.230	011° 10.950	129	129	4,6	28	Micro GI	7	3	31,0	3937	18,0	123	

17:05	54° 34.203	011° 13.626	126	126	4,7	29	Micro GI	7	3	31,0	4114	18,0	122	
17:15							Micro GI	7	3		4199	18,0		GPS Aussetzer
17:25	54° 33.220	011° 15.415	127	127	4,7	29	Micro GI	7	3	31,0	4284	18,0	123	
17:40	54° 32.432	011° 17.187	128	128	4,5	29	Micro GI	9	3	31,0	4420	18		changed shot interval to 9s
17:45	54° 32.287	011° 17.515	128	128	4,8	29	Micro GI	9	3	31,0	4454	18,0	123	
18:05	54° 31.370	011° 19.701	127	128	4,5	29	Micro GI	9	3	31,0	4584	18,0	122	
18:25	54° 30.411	011° 21.743	128	131	4,6	29	Micro GI	9	3	31,0	4724	18,0	119	channel 33 shows strong signal prior to Nutzsignal
18:45	54° 29.548	011° 23.640	128	132	4,6	28	Micro GI	9	3	31,0	4848	18,0	121	
19:05	54° 28.571	011° 25.810	128	131	4,6	27	Micro GI	9	3	31,0	4985	18,0	119	
19:25	54° 27.699	011° 27.790	129	137	4,4	26	Micro GI	9	3	31,0	5114	18,0	119	
19:45	54° 26.629	011° 31.155	126	132	4,5	26	Micro GI	9	3	31,0	5267	18,0	120	
20:03							Micro GI	9	3			18,0		GPS Aussetzer, kommend/gehend zw. 20:03-20:43
20:05	54° 25.730	011° 32.009	127	132	4,7	25	Micro GI	9	3	31,0	5386	18,0	121	
20:25	54° 24.975	011° 33.844	127	133	4,5	25	Micro GI	9	3	30,0	5515	18,0	115	
20:45	54° 24.017	011° 35.999	127	133	4,5	25	Micro GI	9	3	30,0	5651	18,0	114	
21:05	54° 23.146	011° 37.955	127	135	4,7	25	Micro GI	9	3	30,0	5782	18,0	120	
21:25	54° 22.216	011° 40.026	128	137	4,7	25	Micro GI	9	3	30,0	5914	18,0	121	Channel 11 gives strong amplitudes
21:45	54° 21.235	011° 42.252	130	138	4,6	25	Micro GI	9	3	31,0	6050	18,0	119	
22:05	54° 20.309	011° 44.236	128	134	4,5	25	Micro GI	9	3	31,0	6182	18,0	121	
22:25	54° 19.384	011° 46.311	128	131	4,6	25	Micro GI	9	3	30,0	6315	18,0	121	
22:45	54° 18.387	011° 48.560	128	127	4,6	24	Micro GI	9	3	30,0	6465	18,0	119	
23:05	54° 17.437	011° 50.710	128	125	4,4	22	Micro GI	9	3	30,0	6588	18,0	120	
23:10	54° 17.255	011° 51.049	132	133	4,4	22	Micro GI	9	3	30,0	6619	18,0	120	eol 202
23:19	54° 16.696	011° 51.340	203	209	4,5	21	Micro GI	9	3	30,0	6677	18,0	120	sol 203
23:40	54° 15.211	011° 50.008	207	206	4,7	22	Micro GI	9	3	30,0	6821	18,0	120	Line 203 SES data error (error description screenshot on desktop)
00:00	54° 13.901	011° 48.886	207	203	4,7	22	Micro GI	9	3	30,0	6946	18,0	120	
00:20	54° 12.550	011° 47.721	207	201	4,5	22	Micro GI	9	3	30,0	7080	18,0	120	eol 203
00:28	54° 12.331	011° 46.812	297	297	4,6	22	Micro GI	9	3	30,0	7135	18,0	120	sol 204
00:45	54° 12.971	011° 44.836	299	302	4,6	24	Micro GI	9	3	30,0	7250	18,0	120	
01:05	54° 13.736	011° 42.474	299	304	4,6	25	Micro GI	9	3	30,0	7400	18,0	120	
01:25	54° 14.429	011° 40.407	298	300	4,5	25	Micro GI	9	3	30,0	7515	18,0	119	
01:45	54° 15.146	011° 38.163	300	296	4,5	25	Micro GI	9	3	30,0	7652	18,0	120	
02:05	54° 15.933	011° 35.710	291	294	4,8	25	Micro GI	9	3	30,0	7783	18,0	119	
02:25	54° 16.670	011° 33.487	298	302	4,6	24	Micro GI	9	3	30,0	7918	18,0	120	
02:45	54°17.368	011°31.331	298	300	4,8	24	Micro GI	9	3	30,0	8044	18,0	123	
03:05	54°18.148	011°28.945	298	297	4,8	23	Micro GI	9	3	30,0	8177	18,0	120	
03:25	54° 18.921	011° 26.552	298	296	4,7	23	Micro GI	9	3	29,0	8311	18,0	121	
03:45	54° 19.693	011° 24.193	298	296	4,8	22	Micro GI	9	3	29,0	8450	18,0	119	
04:05	54° 20.296	011° 22.325	300	293	4,7	21	Micro GI	9	3	29,0	8550	18,0	122	
04:25	54° 21.321	011° 19.255	299	296	4,6	19	Micro GI	9	3	29,0	8722	18,0	120	
04:28	54° 21.371	011° 19.035	295	287	4,6	18	Micro GI	9	3	29,0	8745	18,0	118	eol 204
04:28	54° 21.371	011° 19.035	295	287	4,6	18	Micro GI	9	3	29,0	8746	18,0	118	sol 205
04:45	54° 20.407	011° 17.889	198	200	4,8	20	Micro GI	9	3	29,0	8858	18,0	118	

05:05	54° 19.118	011° 16.950	203	204	4,8	20	Micro GI	9	3	29,0	8984	18,0	120	
05:25	54° 17.800	011° 15.997	204	203	4,6	19	Micro GI	9	3	29,0	9107	18,0	120	
05:45	54° 16.321	011° 14.937	204	203	4,6	16	Micro GI	9	3	29,0	9240	18,0	120	
06:05	54° 14.809	011° 13.819	204	201	4,6	18	Micro GI	9	3	29,0	9384	18,0	119	
06:25	54° 13.471	011° 12.844	205	201	4,6	17	Micro GI	9	3	29,0	9514	18,0	121	
06:45	54° 12.017	011° 11.788	202	194	4,6	19	Micro GI	9	3	29,0	9646	18,0	121	
07:05	54° 10.787	011° 10.918	205	200	4,7	20	Micro GI	9	3	29,0	9770	18,0	119	
07:25	54° 09.370	011° 09.877	204	201	4,6	22	Micro GI	9	3	30,0	9906	18,0	121	
07:45	54° 07.984	011° 08.858	203	196	4,4	23	Micro GI	9	3	31,0	10029	18,0	120	
08:05	54° 06.550	011° 07.826	204	196	4,5	23	Micro GI	9	3	32,0	10175	18,0	119	
08:25	54° 04.969	011° 06.730	203	200	4,6	23	Micro GI	9	3	31,0	10310	18,0	118	
08:45	54° 03.663	011° 05.746	204	202	4,6	24	Micro GI	9	3	32,0	10439	18,0	119	
09:05	54° 02.295	011° 04.750	203	199	4,7	21	Micro GI	9	3	31,0	10570	18,0	121	
09:07	54° 01.938	011° 94.479	214	215	4,8	17	Micro GI	9	3	31,0	10593	18,0		EOL 205 SOL 206
09:17	54° 01.818	011° 03.315	296	299	4,7	19	Micro GI	9	3	31,0	10674	18,0	119	finished turning
09:25	54° 02.088	011° 02.394	298	300	4,3	24	Micro GI	9	3	31,0	10722	18,0	121	
09:45	54° 02.814	011° 00.021	298	300	4,7	23	Micro GI	9	3	32,0	10856	18,0	121	
10:05	54° 03.556	011° 57.581	298	298	4,7	24	Micro GI	9	3	32,0	10989	18,0	119	
10:25	54° 04.189	011° 55.585	297	294	4,5	22	Micro GI	9	3	32,0	11115	18,0	119	
10:30	54° 04.351	010° 55.996	296	298	4,8	22	Micro GI	9	3	32,0	11153	18,0	119	EOL 206
10:40	54° 04.803	010° 54.814	37	44	4,4	21	Micro GI	9	3	32,0	11204	18,0	119	SOL 207
11:00	54° 06.088	010° 56.780	42	45	4,5	21	Micro GI	9	3	33,0	11349	18,0	121	
11:05	54° 06.382	010° 57.245	43	46	4,5	20	Micro GI	9	3	33,0	11384	18,0	119	
11:25	54° 07.505	010° 59.016	42	45	4,5	19	Micro GI	9	3	34,0	11518	18,0	120	
11:32	54° 07.910	010° 59.694	67	72	4,4	20	Micro GI	9	3	34,0	11569	18,0	119	EOL207
11:41	54° 07.774	010° 00.615	154	150	4,6		Micro GI	9	3	34,0	11623	18,0	121	SOL208
12:05	54° 06.121	011° 01.970	154	149	4,6	24	Micro GI	9	3	33,0	11784	18,0	121	
12:25	54° 04.756	011° 03.100	155	150	4,6	23	Micro GI	9	3	32,0	11915	18,0	121	
12:45	54° 03.390	011° 04.142	150	147	4,5	24	Micro GI	9	3	33,0	12049	18,0	119	
13:05	54° 01.994	011° 05.327	155	150	4,4	14	Micro GI	9	3	32,0	12194	18,0	120	
13:10	54° 01.651	011° 05.647	115	100	3,5	10	Micro GI	9	3	32,0	12220	18,0	122	EOL208
13:14	54° 01.620	011° 05.898	72	69	2,5	10	Micro GI	9	3		12238			End of Mesurement
SES Survey S300														
14:19	54° 03.666	011° 10.366	167	160	3,3		SES							SOL301
14:54	54° 01.853	011° 10.384	234	244	2,7		SES							EOL301
15:04	54° 01.882	011° 09.619	358	5	2,7	5	SES							SOL302
15:40	54° 03.715	011° 09.620	327	320	2,7	12	SES							EOL302, maybe wrong depth
15:49	54° 03.727	011° 08.804	187	171	3,3	12	SES							SOL303
16:25	54° 01.822	011° 08.772	208	231	2,7	20	SES							EOL303
16:34	54° 01.823	011° 08.105	354	3	3,0	18	SES							SOL304
17:10	54° 03.737	011° 08.008	308	294	2,7	23	SES							EOL304
17:20	54° 03.743	011° 07.127	187	172	1,8	24	SES							SOL305
18:00	54° 01.713	011° 07.115	276	278	3,2	12	SES							EOL305

18:10	54° 01.842	011° 06.414	354	10	1,8	12	SES						SOL306
18:48	54° 03.836	011° 06.312	316	287	2,7	25	SES						EOL306
18:58	54° 03.823	011° 05.500	184	167	2,1	25	SES						SOL307
19:37	54° 01.793	011° 05.551	180	184	3,1	12	SES						EOL307
19:45	54° 01.850	011° 04.967	355	4	4,1	15	SES						SOL308
20:22	54° 03.803	011° 04.871	355	349	3,2	25	SES						EOL308
22:35	54° 03.779	011° 03.811	181	169	2,4	24	SES						SOL309
21:16	54° 01.670	011° 04.030	235	259	2,8	16	SES						EOL309
21:24	54° 01.698	011° 03.450	354	3	2,4	17	SES						SOL310
22:07	54° 03.758	011° 02.975	286	247	2,1	24	SES						EOL310
22:17	54° 03.668	011° 02.143	193	151	1,0	21	SES						SOL311
23:03	54° 01.425	011° 02.735	184	203	2,7		SES						EOL311
23:12	54° 01.299	011° 01.949	354	360	3,1		SES						SOL312
23:57	54° 03.538	011° 01.305	347	332	2,8	23	SES						EOL312
00:09	54° 03.354	010° 00.451	179	168	2,9	24	SES						SOL313
00:26	54° 02.483	010° 00.786	169	163	3,1	24	SES						middle of 313
00:53	54° 01.097	011° 01.314	170	189	2,9	21	SES						EOL313
01:03	54° 01.018	011° 00.633	336	338	3,1	23	SES						SOL314
01:25	54° 02.124	011° 00.122	345	347	3,5	24	SES						middle of 314
01:40	54° 02.910	010° 59.738	342	348	2,7	24	SES						EOL314
01:43	54° 02.964	010° 59.857	84	82	3,0	24	SES						SOL315 (west-ost)
02:04	54° 03.215	011° 01.760	77	75	3,3	24	SES						middle of 315
02:22	54°03.448	011°03.442	83	87	3,3	24	SES						EOL315
02:22	54°03.448	011°03.442	83	87	3,3	24	SES						SOL316
02:50	54° 03.455	011°05.890	89	86	3,3	24	SES						
03:24	54°03.476	011°08.922	90	88	3,0	23	SES						EOL316
03:45	54°03.484	011°10.815	95	115	2,8	22	SES						SOL317
03:59	54° 02.776	011°10.685	262	265	3,2	23	SES						middle of 317
04:27	54° 02.661	011°08.071	264	267	3,2	26	SES						EOL317 ,wrong course, stop line
04:43	54° 02.515	011°06.616	264	264	3,3	25	SES						SOL318
05:16	54° 02.782	011°10.707	272	270	2,0	23	SES						
05:37	54° 02.780	011° 08.928	271	271	3,1	24	SES						
06:03	54° 02.778	011° 06.560	269	270	3,2	24	SES						
06:33	54° 02.780	011° 03.998	270	271	3,1	24	SES						
07:24	54° 02.033	010° 59.700	177	168	3,0	24	SES						EOL318
07:41	54° 01.263	011° 00.049	74	64	2,1	23	SES						SOL319
08:14	54° 01.958	011° 02.650	67	61	3,1	25	SES						
08:58	54° 02.182	011° 06.295	91	86	3,0	15	SES						
09:27	54° 02.148	011° 08.843	92	881	3,1	24	SES						
09:49	54° 02.113	011° 10.939	84	45	2,0	23	SES						EOL319
10:14	54° 02.409	011° 08.485	280	285	3,9	26	SES						SOL320
10:34	54° 02.632	011° 06.535	283	288	4,0	26	SES						
10:54	54° 03.042	011° 03.636	289	295	3,6	27	SES						EOL320

11:14	54°03.047	011° 03.356	171	168	3,3	24	SES							SOL321
11:34	54° 02.018	011° 03.576	170	147	2,6	20	SES							EOL321
11:35	54° 02.139	011° 03.835	355	359	3,6	20	SES							SOL322
11:55	54° 03.108	011° 03.713			3,3	25	SES							EOL322
12:07	54° 03.114	011° 04.126	179	171	2,5	24	SES							SOL323
12:26	54° 02.198	011° 04.269	175	170	3,0	20	SES							EOL323
12:30	54° 02.193	011° 04.699	355	357	2,0	21	SES							SOL324
12:50	54° 03.131	011° 04.682	360	360	3,0	25	SES							EOL324
12:56	54° 03.116	011° 05.065	187	180	3,4	25	SES							SOL325
13:14	54° 02.186	011° 05.102	180	171	3,1	19	SES							EOL325
13:19	54° 02.191	011° 05.368	12	8	3,0	18	SES							SOL326
13:38	54° 03.160	011° 05.359	0	357	2,8	25	SES							EOL326
13:43	54°03.140	011° 05.677	179	178	3,7	26	SES							SOL327
13:59	54° 02.214	011°05.712	181	181	3,2	17	SES							EOL327
14:06	54°02.206	011°06.151	13	3	3,7	15	SES							SOL328
14:24	54° 03.119	011° 06.179	6	35	2,9	25	SES							EOL328
14:30	54° 03.066	011° 06.605	176	178	3,5	26	SES							SOL329
14:44	54° 02.186	011° 06.669	169	145	3,6	16	SES							EOL329
14:48	54° 02.215	011°06.890	18	4	3,2	16	SES							SOL330
15:05	54° 03.140	011° 06.922	35	48	3,3	26	SES							EOL330
15:12	54° 03.085	011° 07.350	176	174	3,8	25	SES							SOL331
15:28	54° 02.144	011° 07.490	180	196	3,7	18	SES							EOL331, end of survey
Tuesday, 10.09.2019														
SES Survey S400														
19:13	54° 30.007	010° 00.999	89	90	3,9	24	SES							Start of survey, SOL401
19:24	54° 30.003	010° 02.064	94	114	3,5	22	SES							EOL401
19:27	54° 29.958	010° 02.061	285	275	2,3	24	SES							SOL402
19:39	54° 29.953	010° 00.769	268	256	3,9	24	SES							EOL402
19:43	54° 29.908	010° 00.783	87	86	2,8	24	SES							SOL403
19:54	54° 29.908	010° 02.115	145	188	3,6	24	SES							EOL403
19:57	54° 29.872	010° 02.092	283	273	1,7	24	SES							SOL404
20:09	54° 29.869	010° 00.748	263	240	3,3	24	SES							EOL404
20:12	54° 29.826	010° 00.807	89	90	3,0	24	SES							SOL405
20:24	54° 29.819	010° 02.144	145	186	1,5	24	SES							EOL405
20:28	54° 29.789	010° 02.002	274	267	2,9	23	SES							SOL406
20:39	54° 29.783	010° 00.761	266	240	3,3	24	SES							EOL406
20:42	54° 29.745	010° 00.778	88	89	3,2	24	SES							SOL407
20:53	54° 29.746	010° 02.103	90	91	4,2	23	SES							EOL407, end of survey
Wednesday, 11.09.2019														
SES and MBES Survey S500														
05:06	54°02.16	010°04.63	27	28	4,8	17	SES							Start of survey, SOL 501, SES 4 kHz
05:41	54°04.371	011°06.266	202	204	5,2	23	SES							SOL 502, SES 15 kHz
06:10	54°02.121	011° 04.616	193	170	4,3	18	SES							EOL502

06:16	54° 02.177	011° 04.657	24	22	4,6	21	SES							SOL 503, SES 6kHz
06:44	54°04.315	011° 06.255	28	20	5,2	24	SES							EOL503
08:43	54°02.257	011° 04.750	21	19	4,6	21	SES							SOL504, SES 10kHz, gain angepasst
09:12	54° 04.390	011° 06.297	1	359	4,6	24	SES							EOL 504
09:37	54° 03.021	011° 05.284	204	208	4,7	25	SES							SOL 505, SES 8kHz (zu spät eingeschaltet)
09:49	54° 02.131	011° 04.639	180	163	4,0	19	SES							EOL 505 (nicht vollständig)
09:53	54° 02.197	011° 04.678	27	29	5,1	21	SES							SOL 506, SES 8kHz
10:21	54°04,37	011°06,31	57	52	4,0	23	SES							EOL 506
10:39							MBES							Multibeam survey
11:18	54° 02.268	011° 04.739	27	28	4,2	21	SES							SOL 507, SES 12kHz
11:51	54° 04.328	011° 06.265	14	341	3,0	23	SES							EOL 507
11:57	54°04.28	011°06.23	203	209	3,5	27	SES							SOL 508, SES 5kHz
	54°	011°					SES							EOL 508
Seismic Survey S600														
15:11	54°03.227	011°04.981	74	69	4,1	24	Micro G	8	3	19,0	13000	18	120	start recording 6 section 48 channels, channel 11,16,33 seems to be dead; parallel recording Innomar, run up to profile; streamer offset +3 m
15:21	54°03.748	011° 07.892	71	70	4,1	23	Micro G	7	3	26,0	13117	18		changed shotinterv. to 7s
15:31	54° 04.048	011° 09.331	68	69	4,3	23	Micro G	7	3	28,0	13215	18	118	
15:49	54°04.473	011° 10.930	56	55	4,3	22	Micro G	7	3	28,0	13359	18	120	SOL601
16:00	54° 04.865	011° 11.923	55	52	4,1	24	Micro G	7	3	29,0	13439	18	120	
16:20	54° 05.725	011° 13.815	54	49	4,2	23	Micro G	7	3	29,0	13618	18	120	
16:40	54° 06.524	011° 15.666	51	50	4,1	20	Micro G	7	3	29,0	13790	18	119	
17:00	54°07.364	011° 17.550	55	57	4,3	20	Micro G	7	3	29,0	13964	18	120	
17:20	54°08.238	011° 19.520	53	55	4,0	22	Micro G	7	3	29,0	14142	18	120	
17:40	54° 09.081	011° 21.405	52	53	4,1	24	Micro G	7	3	29,0	14313	18	120	
18:00	54° 09.804	011° 23.067	54	54	3,9	24	Micro G	7	3	30,0	14472	18	119	
18:20	54° 10.786	011° 25.317	53	50	4,4	23	Micro G	7	3	30,0	14668	18	115	
18:40	54° 11.573	011° 27.046	53	49	4,6	23	Micro G	7	3	30,0	14817	18		
18:42	54° 11.654	011° 27.241	22	21	4,2	23	Micro G	7	3	29,0	14830	18	118	EOL601 SOL602
19:00	54° 12.905	011° 28.416	27	21	4,2	22	Micro G	7	3	29,0	15007	18	119	Checking on the compressor. Slight change of course due to strong winds
19:20	54° 29.548	011° 29.552	26	14	4,3	22	Micro G	7	3	29,0	15171	18	120	
19:35	54° 15.061	011° 30.428	18	356	3,7	23				29,0	15291			End of Mesurement
SES Survey S700														
20:18	54° 13.344	011° 25.174	241	241	7,2	22	SES							Transit
21:45	54° 08.737	011° 07.143	320	322	4,6	21	SES							SOL701 Star of Survey with 8 khz
22:09	54°10.691	011°06.001	328	290	3,9	13	SES							EOL701
22:18	54° 10.301	011° 05.425	164	171	5,0	16	SES							SOL702
22:40	54° 08.436	011° 06.626	175	211	3,3	22	SES							EOL702
22:49	54° 08.171	011° 05.946	337	328	5,5	21	SES							SOL703
23:14	54° 10.118	011° 04,604	279	233	2,0	14	SES							EOL703
23:22	54° 09.76	011° 04.069	161	171	5,0	16	SES							SOL704

23:46	54° 07.78	011° 05.33	177	218	3,1	22	SES							EOL704
	54°	011°					SES							SOL705
00:22	54° 09.825	011° 03.182			3,0	14	SES							EOL705 writing error
00:54	54° 07.57	011° 04.67	342	333	3,9	21	SES							SOL705 repeat line because of lost data
01:22	54° 09.792	011° 03.27	328	290	3,1	14	SES							EOL705
01:31	54° 09.44	011° 02.76	165	170	4,8	18	SES							SOL706
01:53	54° 07.60	011° 03.74	163	166	5,0	22	SES							EOL706
02:04	54° 07.515	011° 02.995	339	339	5,3	22	SES							SOL707
02:28	54° 09.409	011° 02.031	325	296	3,8	13	SES							EOL707
02:34	54° 09.223	011° 01.450	163	167	5,3	15	SES							SOL708
02:59	54° 07.230	011°02.388	163	187	4,6	19	SES							EOL708
03:06	54° 06.987	011° 01.717	335	333	5,3	21	SES							SOL709
03:31	54° 08.971	011° 00.616	314	269	2,9	16	SES							EOL709
03:40	54° 08.692	011° 59.797	158	162	4,2	14	SES							SOL710
04:13	54° 06.041	011° 01.249	162	180	4,8	24	SES							EOL710
04:21	54° 05.767	011° 00.626	162	336	5,3	23	SES							SOL711
04:49	54° 08.094	011° 59.187	322	300	4,5	15	SES							EOL711
04:58	54°07.779	010° 58.571	155	161	5,2	13	SES							SOL712
05:27	54° 05.474	010° 59.953	159	162	5,2	22	SES							EOL712
05:35	54° 05.283	010° 59.285	333	326	5,0	22	SES							SOL713
06:02	54° 07.324	010° 57.632	253	222	2,0	11	SES							EOL713, Fehlermeldung: kein Back-Up File
06:12	54° 06.781	010° 57.286	158	159	4,5	12	SES							SOL714
06:36	54° 04.979	010° 58.957	167	200	4,1	22	SES							EOL714
06:46	54° 04.727	010° 58.001	335	322	4,1	22	SES							SOL715
07:09	54° 06.462	010° 56.558	260	230	2,4	13	SES							EOL715
07:17	54° 06.101	010° 56.130	166	170	3,7	17	SES							SOL716
07:40	54° 04.426	010° 57.350	157	164	4,8	22	SES							EOL716, end of profile
07:43	54° 04.284	010° 57.668	106	107	8,6	22	SES							SOL717, transit to gravity coring location
08:09	54° 02.938	011° 04.039	225	229	2,0	24	SES							EOL717
								Thursday, 12.09.2019						
								Seismic sSurvey and SES Survey S800						
13:22	54° 11.22	011° 26.83	41	29	3,7	23	Micro G	7	3	20,0	16000	18	50	SO800 start of soft start, 6 Sections 48 channels
13:30	54° 11.71	011° 27.32	29	21	2,8	23	Micro G	7	3	23,0	16058	18	80	
13:41	54° 12.31	011° 27.90	28	19	4,1		Micro G	7	3	26,0	16134	18	100	
13:50	54° 12.88	011° 28.42	27	18	4,0		Micro G	7	3	27,0	16217	18	120	SOL801
14:10	54° 14.04	011° 29.5	32	23	4,2		Micro G	7	3	29,0	16389	18	120	
14:30	54° 15.27	011° 30.62	28	25	4,1		Micro G	7	3	29,0	16560	18	121	
14:50	54° 16.428	011° 31.678	28	27	3,9	23	Micro G	7	3	30,0	16727	18	120	
15:10	54° 17.750	011° 32.925	28	23	3,9	24	Micro G	7	3	30,0	16920	18	120	
15:30	54° 18.939	011° 34.031	28	21	4,0	25	Micro G	7	3	30,0	17090	18	120	
15:50	54° 20.102'	011° 35.097	29	21	4,1	25	Micro G	7	3	30,0	17250	18	128	gun pressure increased
16:08	54° 21.242	011° 36.188	35	25	3,8	25	Micro G	7	3	30,0	17412	18	128	EOL 801 SOL 802
16:30	54° 21.506	011° 38.702	88	74	4,1	25	Micro G	7	3	31,0	17590	18	129	

16:50	54° 21.506	011° 41.144	92	83	4,0	25	Micro G	7	3	31,0	17770	18	129	
17:10	54° 21.495	011°43.326	89	86	4,3	25	Micro G	7	3	31,0	17935	18	130	
17:30	54° 21.505	011° 45.700	92	97	4,1	24	Micro G	7	3	31,0	18102	18	130	
17:50	54° 21.524	011° 48.245	90	96	4,0	23	Micro G	7	3	31,0	18289	18	130	
18:12	54° 21.502	011° 50.642	91	94	4,1	21	Micro G	7	3	31,0	18471	18	124	
18:32	54° 21.507	011° 53.061	88	92	4,0	20	Micro G	7	3	31,0	18640	18	130	
18:53	54° 21.508	011° 55.452	90	93	4,0	19	Micro G	7	3	30,0	18821	18	130	
19:09	54° 21.500	011° 57.100	89	92	4,2	18	Micro G	7	3	30,0	18948	18	124	
19:21	54° 21.503	011° 58.651	98	105	4,0	18	Micro G	7	3	30,0	19059	18	130	EOL 802 SOL803
19:47	54° 20.06	011° 58.85	195	203	4,2	18	Micro G	7	3	30,0	19274	18	125	
20:10	54° 18.478	011° 58.155	194	200	4,0	18	Micro G	7	3	30,0	19485	18	125	
20:35	54° 16.804	011° 57.399	195	201	4,1	18	Micro G	7	3	30,0	19701	18	130	
20:53	54° 15.643	011° 56.874	195	200	4,2	19	Micro G	7	3	30,0	19853	18	130	
21:00	54° 15.091	011° 56.630	197	295	4,2	18	Micro G	7	3	30,0	19906	18	130	
Friday, 13.09.2019														
SES Survey S900														
11:50	54° 34.840	011° 04.799	208	223	4,8	24	SES							SOL901, starting Innomar Survey
12:07	54° 33.680	011° 03.459	191	169	5,1	12	SES							EOL901
12:16	54° 33.997	011° 04.676	102	113	5,9	13	SES							SOL902
12:30	54° 33.642	011° 06.647	124	161	3,5	16	SES							EOL902
12:34	54° 33.682	011° 06.583	18	344	2,8	18	SES							SOL903
12:39	54° 34.159	011° 06.384	290	280	7,7	22	SES							EOL903 SOL904
12:48	54° 34.594	011° 04.043	276	164	8,6	20	SES							EOL904 Innomar stay activated
13:01	54° 34.288	011° 00.341	262	261	11,1	13	SES							End of profil

11 List of Stations

Activity - Device Operation	Timestamp	Device	Action	Latitude	Longitude	Comment
AL527_42-1	13.09.2019 11:30	Grab	on deck	54°34,298' N	011°04,174' E	
AL527_42-1	13.09.2019 11:29	Grab	in the water	54°34,300' N	011°04,179' E	Al527_Gr11
AL527_41-1	13.09.2019 11:17	Grab	on deck	54°34,415' N	011°04,310' E	
AL527_41-1	13.09.2019 11:16	Grab	in the water	54°34,420' N	011°04,308' E	Al527_Gr10
AL527_40-1	13.09.2019 11:04	CTD	on deck	54°34,550' N	011°04,495' E	
AL527_40-1	13.09.2019 11:01	CTD	in the water	54°34,562' N	011°04,478' E	
AL527_39-1	13.09.2019 10:59	Grab	on deck	54°34,562' N	011°04,477' E	
AL527_39-1	13.09.2019 10:58	Grab	in the water	54°34,564' N	011°04,480' E	Al527_Gr09
AL527_38-1	13.09.2019 10:40	Grab	on deck	54°34,738' N	011°04,697' E	
AL527_38-1	13.09.2019 10:38	Grab	in the water	54°34,740' N	011°04,698' E	Al527_Gr08
AL527_37-1	13.09.2019 01:12	CTD	on deck	54°34,756' N	011°05,818' E	
AL527_37-1	13.09.2019 01:10	CTD	in the water	54°34,771' N	011°05,660' E	
AL527_36-1	13.09.2019 10:38	Multibeam	in Moonpool	54°34,740' N	011°04,699' E	
AL527_36-1	13.09.2019 10:34	Multibeam	out Moonpool	54°34,739' N	011°04,741' E	
AL527_36-1	13.09.2019 10:25	Multibeam	profile end	54°34,602' N	011°04,811' E	
AL527_36-1	13.09.2019 01:32	Multibeam	profile start	54°34,772' N	011°04,221' E	
AL527_36-1	13.09.2019 00:54	Multibeam	in Moonpool	54°34,850' N	011°05,225' E	
AL527_35-1	12.09.2019 21:10	Seismic Source	Airgun on deck	54°14,760' N	011°56,077' E	
AL527_35-1	12.09.2019 21:00	Seismic Source	profile end	54°15,115' N	011°56,648' E	
AL527_35-1	12.09.2019 13:29	Seismic Source	profile start	54°11,682' N	011°27,279' E	
AL527_35-1	12.09.2019 13:12	Seismic Source	Airgun in water	54°10,857' N	011°26,126' E	
AL527_34-1	12.09.2019 21:15	Seismic Towed Receiver	Streamer on deck	54°14,626' N	011°55,758' E	
AL527_34-1	12.09.2019 13:06	Seismic Towed Receiver	Streamer in water	54°10,703' N	011°25,838' E	
AL527_33-1	12.09.2019 10:50	Gravity Corer	on deck	54°02,610' N	011°05,369' E	
AL527_33-1	12.09.2019 10:44	Gravity Corer	in the water	54°02,626' N	011°05,372' E	Al527_GC07
AL527_32-1	12.09.2019 10:21	Gravity Corer	on deck	54°02,410' N	011°04,695' E	
AL527_32-1	12.09.2019 10:15	Gravity Corer	in the water	54°02,422' N	011°04,674' E	2nd try
AL527_32-1	12.09.2019 10:09	Gravity Corer	on deck	54°02,443' N	011°04,672' E	empty
AL527_32-1	12.09.2019 10:02	Gravity Corer	in the water	54°02,464' N	011°04,664' E	Al527_GC06
AL527_31-1	12.09.2019 09:16	Gravity Corer	on deck	54°02,671' N	011°04,750' E	

AL527_31-1	12.09.2019 09:10	Gravity Corer	in the water	54°02,679' N	011°04,718' E	Al527_GC05
AL527_30-1	12.09.2019 08:50	Gravity Corer	on deck	54°02,331' N	011°04,285' E	Umgefallen
AL527_30-1	12.09.2019 08:44	Gravity Corer	in the water	54°02,346' N	011°04,277' E	Al527_GC04
AL527_29-1	12.09.2019 08:21	Gravity Corer	on deck	54°02,811' N	011°04,180' E	
AL527_29-1	12.09.2019 08:15	Gravity Corer	in the water	54°02,823' N	011°04,167' E	Al527_GC03
AL527_28-1	12.09.2019 07:40	SES2000	profile end	54°04,386' N	010°57,372' E	
AL527_28-1	11.09.2019 21:45	SES2000	profile start	54°08,767' N	011°07,117' E	
AL527_27-2	11.09.2019 19:40	Seismic Source	Airgun on deck	54°15,345' N	011°30,398' E	
AL527_27-2	11.09.2019 19:34	Seismic Source	profile end	54°15,088' N	011°30,424' E	
AL527_27-2	11.09.2019 15:48	Seismic Source	profile start	54°04,445' N	011°10,861' E	
AL527_27-2	11.09.2019 14:45	Seismic Source	Airgun in water	54°02,996' N	011°05,168' E	
AL527_27-1	11.09.2019 19:46	Seismic Towed Receiver	Streamer on deck	54°15,360' N	011°30,087' E	
AL527_27-1	11.09.2019 14:40	Seismic Towed Receiver	Streamer in water	54°03,078' N	011°05,317' E	
AL527_26-1	11.09.2019 14:25	Grab	on deck	54°03,243' N	011°05,509' E	Al527_Gr07
AL527_26-1	11.09.2019 14:24	Grab	in the water	54°03,244' N	011°05,514' E	
AL527_25-1	11.09.2019 14:12	Grab	on deck	54°02,650' N	011°05,058' E	Al527_Gr06
AL527_25-1	11.09.2019 14:10	Grab	in the water	54°02,662' N	011°05,054' E	
AL527_24-1	11.09.2019 14:03	Grab	on deck	54°02,390' N	011°04,901' E	Al527_Gr05
AL527_24-1	11.09.2019 14:01	Grab	in the water	54°02,397' N	011°04,893' E	
AL527_23-1	11.09.2019 13:49	Grab	on deck	54°02,374' N	011°04,827' E	Al527_Gr04
AL527_23-1	11.09.2019 13:47	Grab	in the water	54°02,374' N	011°04,826' E	
AL527_22-1	11.09.2019 13:33	Grab	on deck	54°02,331' N	011°04,762' E	Al527_Gr03
AL527_22-1	11.09.2019 13:31	Grab	in the water	54°02,337' N	011°04,765' E	
AL527_21-1	11.09.2019 13:11	Grab	on deck	54°02,275' N	011°04,727' E	AL527_Gr02
AL527_21-1	11.09.2019 13:09	Grab	in the water	54°02,273' N	011°04,729' E	
AL527_20-1	11.09.2019 12:55	Grab	on deck	54°02,179' N	011°04,670' E	Al527_Gr01
AL527_20-1	11.09.2019 12:54	Grab	in the water	54°02,169' N	011°04,686' E	
AL527_19-2	11.09.2019 11:28	Multibeam	out Moonpool	54°02,900' N	011°05,205' E	
AL527_19-2	11.09.2019 11:26	Multibeam	profile end	54°02,816' N	011°05,144' E	
AL527_19-2	11.09.2019 10:39	Multibeam	profile start	54°04,178' N	011°06,166' E	
AL527_19-2	11.09.2019 10:27	Multibeam	in Moonpool	54°04,304' N	011°06,249' E	
AL527_19-1	11.09.2019 12:37	SES2000	profile end	54°02,028' N	011°04,636' E	
AL527_19-1	11.09.2019 08:42	SES2000	profile start	54°02,173' N	011°04,677' E	
AL527_18-1	11.09.2019 08:09	Gravity Corer	on deck	54°02,738' N	011°05,529' E	Al527_GC02

AL527_18-1	11.09.2019 08:02	Gravity Corer	in the water	54°02,739' N	011°05,520' E	
AL527_17-1	11.09.2019 07:17	Gravity Corer	on deck	54°02,676' N	011°04,710' E	Al527_GC01
AL527_17-1	11.09.2019 07:11	Gravity Corer	in the water	54°02,680' N	011°04,694' E	
AL527_16-1	11.09.2019 06:43	SES2000	profile end	54°04,351' N	011°06,284' E	
AL527_16-1	11.09.2019 05:00	SES2000	profile start	54°02,097' N	011°05,056' E	
AL527_15-1	10.09.2019 20:53	SES2000	profile end	54°29,747' N	010°02,105' E	
AL527_15-1	10.09.2019 19:13	SES2000	profile start	54°30,010' N	010°00,848' E	
AL527_14-1	10.09.2019 17:07	Hydrosonde	on deck	54°30,065' N	010°00,746' E	
AL527_14-1	10.09.2019 17:03	Hydrosonde	in the water	54°30,067' N	010°00,750' E	
AL527_13-1	10.09.2019 18:59	Multibeam	out Moonpool	54°29,853' N	010°02,067' E	
AL527_13-1	10.09.2019 18:53	Multibeam	profile end	54°29,745' N	010°02,039' E	
AL527_13-1	10.09.2019 17:07	Multibeam	profile start	54°30,064' N	010°00,746' E	
AL527_13-1	10.09.2019 15:50	Multibeam	in Moonpool	54°32,003' N	010°02,743' E	
AL527_12-1	10.09.2019 15:23	Underwater Video System	on deck	54°31,975' N	010°02,462' E	
AL527_12-1	10.09.2019 12:20	Underwater Video System	in the water	54°32,159' N	010°02,733' E	
AL527_11-1	10.09.2019 06:20	Multibeam	out Moonpool	54°25,790' N	010°11,066' E	
AL527_11-1	10.09.2019 06:18	Multibeam	profile end	54°25,797' N	010°10,889' E	
AL527_11-1	10.09.2019 05:43	Multibeam	profile start	54°26,019' N	010°11,348' E	
AL527_11-1	10.09.2019 05:30	Multibeam	in Moonpool	54°26,224' N	010°11,778' E	
AL527_10-1	09.09.2019 18:50	Hydrosonde	on deck	54°02,780' N	011°04,075' E	
AL527_10-1	09.09.2019 18:45	Hydrosonde	in the water	54°02,798' N	011°04,081' E	
AL527_9-1	09.09.2019 16:15	Hydrosonde	on deck	54°02,843' N	011°04,209' E	
AL527_9-1	09.09.2019 16:12	Hydrosonde	in the water	54°02,839' N	011°04,205' E	
AL527_8-1	09.09.2019 21:44	Multibeam	out Moonpool	54°02,499' N	011°06,054' E	
AL527_8-1	09.09.2019 21:43	Multibeam	profile end	54°02,499' N	011°06,016' E	
AL527_8-1	09.09.2019 14:26	Multibeam	profile start	54°03,159' N	011°06,332' E	
AL527_8-1	09.09.2019 14:01	Multibeam	in Moonpool	54°02,122' N	011°05,768' E	
AL527_7-1	09.09.2019 13:26	SES2000	profile end	54°02,540' N	011°05,371' E	
AL527_7-1	08.09.2019 12:18	SES2000	profile start	54°05,198' N	011°02,721' E	
AL527_6-2	08.09.2019 13:27	Seismic Towed Receiver	Streamer on deck	54°01,806' N	011°06,287' E	
AL527_6-2	08.09.2019 13:13	Seismic Towed Receiver	profile end	54°01,614' N	011°05,831' E	
AL527_6-2	08.09.2019 04:27	Seismic Towed Receiver	alter course	54°21,342' N	011°19,149' E	

AL527_6-2	07.09.2019 15:48	Seismic Towed Receiver	alter course	54°37,481' N	011°05,157' E	
AL527_6-2	07.09.2019 13:05	Seismic Towed Receiver	profile start	54°32,642' N	010°45,292' E	
AL527_6-2	07.09.2019 12:44	Seismic Towed Receiver	Streamer in water	54°32,254' N	010°43,131' E	
AL527_6-1	08.09.2019 13:20	Seismic Source	Airgun on deck	54°01,713' N	011°06,145' E	
AL527_6-1	07.09.2019 12:37	Seismic Source	Airgun in water	54°32,229' N	010°42,693' E	
AL527_5-1	07.09.2019 05:31	Hydrosonde	on deck	54°31,992' N	010°02,393' E	
AL527_5-1	07.09.2019 05:28	Hydrosonde	in the water	54°31,995' N	010°02,385' E	
AL527_4-1	06.09.2019 20:31	Seismic Source	Airgun on deck	54°31,890' N	010°08,997' E	
AL527_4-1	06.09.2019 20:13	Seismic Source	Airgun in water	54°32,147' N	010°08,211' E	Gerätetest
AL527_3-2	06.09.2019 18:47	Seismic Source	Airgun on deck	54°32,108' N	010°08,630' E	Airgun defekt
AL527_3-2	06.09.2019 17:19	Seismic Source	Airgun in water	54°31,883' N	010°03,670' E	
AL527_3-1	06.09.2019 18:56	Seismic Towed Receiver	Streamer on deck	54°32,084' N	010°09,302' E	
AL527_3-1	06.09.2019 18:38	Seismic Towed Receiver	profile end	54°32,110' N	010°08,160' E	Unterbrech-ung Airgun defekt
AL527_3-1	06.09.2019 17:53	Seismic Towed Receiver	profile start	54°32,196' N	010°03,058' E	
AL527_3-1	06.09.2019 17:09	Seismic Towed Receiver	Streamer in water	54°32,099' N	010°03,858' E	
AL527_2-1	06.09.2019 15:18	Hydrosonde	on deck	54°31,682' N	010°02,050' E	
AL527_2-1	06.09.2019 15:15	Hydrosonde	in the water	54°31,678' N	010°02,055' E	
AL527_1-1	07.09.2019 10:12	Multibeam	out Moonpool	54°32,078' N	010°02,802' E	
AL527_1-1	07.09.2019 10:10	Multibeam	profile end	54°32,128' N	010°02,901' E	
AL527_1-1	06.09.2019 23:34	Multibeam	profile start	54°30,071' N	010°01,485' E	
AL527_1-1	06.09.2019 17:02	Multibeam	profile end	54°32,189' N	010°03,721' E	
AL527_1-1	06.09.2019 09:07	Multibeam	profile start	54°31,512' N	010°03,384' E	
AL527_1-1	06.09.2019 08:49	Multibeam	in Moonpool	54°31,602' N	010°03,368' E	